Received 3 July 2024; accepted 26 July 2024. Date of publication 29 July 2024; date of current version 9 August 2024.

\*Digital Object Identifier 10.1109/OJCOMS.2024.3435704\*

# Securing Full-Duplex Cognitive Radio With Reconfigurable Intelligent Surfaces via Coordinated Beamforming and Power Control

A. ABDELAZIZ SALEM<sup>®</sup> 1,2, MAHMOUD H. ISMAIL<sup>®</sup> 2,3 (Senior Member, IEEE),
AND AHMED S. IBRAHIM<sup>®</sup> 4 (Senior Member, IEEE)

<sup>1</sup>Department of Electronics and Electrical Communications Engineering, Menoufia University, Shebin El Kom 6131567, Egypt

<sup>2</sup>Department of Electrical Engineering, American University of Sharjah, Sharjah, UAE

<sup>3</sup>Department of Electronics and Communications Engineering, Faculty of Engineering, Cairo University, Giza 12613, Egypt
<sup>4</sup>Electrical and Computer Engineering Department, Florida International University, Miami, FL 33174, USA

CORRESPONDING AUTHOR: M. H. ISMAIL (e-mail: mhibrahim@aus.edu)

The work of A. Abdelaziz Salem and Mahmoud H. Ismail was supported by the American University of Sharjah through Faculty Research
Grant under Grant FRG22-C-E13 and Grant FRG23-C-E12. The work of Ahmed S. Ibrahim was supported in part
by the National Science Foundation under Award CNS-2144297.

ABSTRACT This paper addresses the unexplored challenge of achieving secure communication in a full-duplex (FD) cognitive radio (CR) system employing a reconfigurable intelligent surface (RIS) where a passive eavesdropper (Eve) is equipped with multiple antennas. The secondary base station (SBS), operating in full-duplex mode, serves as an uplink (UL) communication provider for secondary users (SUs) while actively launching a jamming signal against Eve to degrade its downlink (DL) interception capability, thus aiding the primary network. This study faces several technical challenges. First, complex interference management arises as the FD-SBS must manage interference between UL communications and active jamming signals to ensure both secure communication and minimal interference to legitimate users. Additionally, optimizing multi-dimensional beamforming across the primary base station (PBS) DL, the FD-SBS jamming, the passive RIS, and the UL communication power imposes substantial complexities due to conflicting objectives and constraints. To this end, we propose a coordinated beamforming approach, which maximizes the minimum secrecy rate with a minimum target rate for the UL SUs, a maximum DL PBS transmission power, jamming power limits and RIS unit modulus constraints. To address the problem non-convexity, it is decomposed into four sub-problems, which are solved via employing semidefinite programming (SDP) and successive convex approximation (SCA) based alternating optimization. Simulation results show the effectiveness of RIS phase shift optimization to enhance secrecy performance, how much jamming power is needed to keep balance between the secrecy performance and the UL communication service, as well as the effectiveness of the proposed solution against various benchmarks.

INDEX TERMS Reconfigurable intelligent surfaces (RIS), full-duplex cognitive radio systems, multi-user single-input and multiple-output (MU-SIMO), coordinated beamforming, alternative optimization.

# I. INTRODUCTION

WITH the exponential growth of wireless applications, the radio spectrum scarcity became a bottleneck for achieving high data rate communication. *Cognitive radio* (CR) technology has been proposed to alleviate the *spectrum* 

scarcity issue [1]. The main concept behind CR is to offer access for unlicensed secondary users (SUs) within the licensed spectrum of primary users (PUs). Specifically, the spectrum vacancies of PUs can be allocated for SUs in an opportunistic access mode, or both PUs and SUs could be

allowed to access the same spectrum concurrently in an underlay mode as long as the interference from the SUs has a tolerable impact on the PUs [2].

In spite of its advantages, spectrum sharing in underlay CR systems, e.g., cognitive satellite terrestrial network (CSTN) [3], [4], poses a security threat since the existence of eavesdroppers (Eve) in the vicinity of PUs and/or SUs leads to a high probability of interception [5]. As a result, Physical layer security (PLS) in CR networks has been widely investigated to provide secure data transmission in wireless networks via degrading the wireless channel of Eve [6], [7], [8], [9], [10], [11], [12]. More recently, reconfigurable intelligent surfaces (RISs) have also been exploited for improving communication in environments with severe blockages [13], enabling simultaneous wireless information and power transfer [14], and enhancing PLS [15]. Focusing on security aspects, the radio environment can be artificially manipulated to degrade Eve's channel while improving the legitimate channels.

In the dynamically changing wireless world, CR technology stands out by allowing spectrum sharing between primary and secondary networks, hence significantly improving the spectral efficiency. However, this shared environment inherently increases vulnerability to eavesdropping, especially against a potential Eve that possesses the capability to decode legitimate signals with multiple antennas, thus enjoying a higher degree of freedom in intercepting communications. This scenario poses a critical question: How can one exploit the secondary network to minimize the harm caused by possible eavesdropping on the primary one, while ensuring the continuous functioning of the secondary network? More specifically, how may the secondary network "return the favor" of using the shared spectrum by cooperating in an underlay mode to secure the primary communication via passive beamforming enabled by a reconfigurable intelligent surface?

In this paper, we aim to further enhance the PLS of RISassisted CR network by considering a dual functionality for SBS. More specifically we propose for SBS to operate in a full-duplex (FD) mode, by launching an active jamming (AJ) signal against a potential eavesdropper to degrade their ability to intercept the downlink (DL) service being provided to the PUs. So on one hand and thanks to the PBS, the fullduplex (FD)-SBS serves its SUs with their corresponding Quality of Service (QoS) requirements. On the other hand, the FD-SBS returns the favor to the PBS by jamming interference against Eve. However, full duplex mode at FD-SBS results in self-interference, and this is the first challenge in this paper. We point out that deploying FD-SBS in the discussed context has not been explored in the literature before. The second challenge in this paper is considering the scenario where Eve is equipped with multiple antennas, while all other users have single antennas. Such scenario makes PLS more challenging as the CR users have fewer degrees of freedom compared. To simultaneously address the two aforementioned challenges, this paper focuses on joint beamforming among the FD-SBS, the RIS, and the PBS to secure the CR network operation.

Specifically in this paper, we formulate a minimum (worst-case) secrecy rate maximization (MSRM) problem, in which the AJ beamforming matrix at the FD-SBS, the UL transmit power of the SUs, the DL beamformers at the PBS, the UL receive beamforming and RIS reflection coefficients are jointly optimized. This is achieved while taking into account the minimum target UL rate for the SUs, the maximum allowed transmission power for the DL PBS, an upper limit on the jamming power, and UL transmission power as well as the RIS unit modulus constraint to keep the balance between the DL secrecy rate maximization of PUs and rate requirements for the SUs. The formulated MSRM problem is *non-convex* due to the high coupling between the decision variables.

We propose to solve the non-convex MSRM problem by dividing it into four convex sub-problems, which are alternatingly solved. The first one targets maximizing the UL rate of the SUs by deriving a closed-form expression for the optimal UL receive beamformers at the SBS. In the second one, we jointly design the DL beamformers for the PUs, at the PBS, and the AJ beamforming vector, at the FD-SBS. In the third sub-problem, we optimize the transmit power of the UL SUs to ensure controlled interference on the DL primary network. Finally, the phase shifts of the RIS elements are optimized in the fourth sub-problem. We adopt semidefinite programming (SDP) and successive convex approximation (SCA) to design the PBS, AJ and RIS beamformers as will be shown in the sequel.

Specifically, the key contributions of this paper, in comparison to the state-of-the-art, are clearly highlighted in Table 1. To elaborate further:

- Assuming a potential Eve that has the capability to perform signal combining with multiple antennas, we jointly design a jamming beamforming matrix at the FD-SBS, the UL transmit power of the SUs, the DL beamformers at the PBS, the UL receive beamforming and RIS passive beamformers to maximize the minimum secrecy rate of a primary network while ensuring the UL communication QoS requirement for the secondary network.
- Introducing an alternating optimization (AO) algorithm, which achieves the convergence for the four subproblems.

The remaining part of this paper is organized as follows: The system model is presented in Section III. The problem of MSRM is formulated and solved in Section IV. Numerical results are then presented and discussed in Section V before the paper is finally concluded in Section VI.

*Notations:* lowercase boldface and uppercase boldface letters are used to denote vectors and matrices, respectively, while the normal face letters are used for scalars. Mathematical fonts, e.g.,  $\mathcal{B}$  are dedicated for set notation.  $\mathbb{C}^{N\times M}$ , diag(.),  $I_N$  and Tr(.) denote the  $N\times M$  complex space,

TABLE 1. Emphasizing our distinctive contributions compared to the most relevant state-of-the-art.

|                         | This paper | [12]     | [2]       | [5]       | [16]   | [17]      | [18]   | [19]   |
|-------------------------|------------|----------|-----------|-----------|--------|-----------|--------|--------|
| RIS/Relay               | ✓          |          | ✓         | ✓         | ✓      |           | Relay  |        |
| FD-SBS/PBS              |            |          |           |           |        |           |        | FD-PU  |
| UL and DL transmission  | DL         | DL       | DL        | DL        | DL     | DL        | ✓      | DL     |
| Eve with multi-antennas | ✓          |          | Multi-Eve | Multi-Eve |        | Multi-Eve | ✓      |        |
| Jamming/AN source       | FD-SBS     | UAV      |           |           | SBS    | SBS       | UAV    | FD-PU  |
| PUs                     | Multiple   | Multiple | Single    | Single    | Single | Multiple  | Single | Single |
| SUs                     | Multiple   | Multiple | Single    | Single    | Single | Single    | Single | Single |
| Metric                  | MSRM       | ASR      | SR        | SR        | SR     | PM        | SEEM   | SOP    |

ASR: Average secrecy rate

SEEM: Secrecy energy efficiency maximization

PM: Power minimization SOP: Secrecy outage probability

the diagonal matrix with the elements of the input vector on its main diagonal, the unit matrix with dimensions  $N \times N$  and the trace operator, respectively. The notations  $\mathbf{X} \succeq 0$ ,  $\mathbf{X}^T, \mathbf{X}^*$  and  $\mathbf{X}^H$  denote the Hermitian positive semidefinite property, transpose, conjugate and the conjugate transpose of the matrix  $\mathbf{X}$ , respectively.

### **II. RELATED WORK**

In is section, we highlight some recent works that tackled the security challenge in underlay CR networks from the PLS point of view as well as using RISs.

PLS in CR networks has been widely investigated in [7], [8], [9], [10], [11], [12]. In this context, artificial noise (AN) and beamforming were jointly optimized to enhance the security of the primary and secondary networks in [7]. In addition, authors of [8] optimized the jamming beamforming based on the null space of the legitimate PUs' channels.

Motivated by the concept of cooperative communication, [9] exploited AN to jam the eavesdroppers to maximize the secrecy rate (SR) of the secondary network while maintaining the SR constraints of the PUs. Also, in [10], an unmanned aerial vehicle (UAV) was used as a friendly jammer to enhance the secrecy performance of the SUs via jointly optimizing the UAV trajectory and transmission power. Finally, motivated by SR maximization, the authors of [11] and [12] studied secure operation of primary and secondary networks, respectively. It is notable that the studies [7], [8], [9], [10], [11], [12] not only adopted an additional jamming power, but also considered a relatively large number of antennas at the secondary base station to improve the secrecy performance of the CR system.

RISs have been proposed as a revolutionary solution for improving the performance of wireless networks in general [20]. Unlike active relays, RISs are able to reflect the incident signal without additional signal processing [21]. Quite a few studies have considered the use of RISs for security improvement in CR networks. For example, considering the concept of secrecy energy efficiency (SEE), the trade-off between achievable SR and energy efficiency has been studied in [2], where beamforming at a secondary base station (SBS) and an RIS were designed considering perfect channel state information (CSI) of the eavesdroppers.

Motivated by the estimation mismatch of Eve's CSI in a millimeter wave (mmWave) CR system, Wu et al. proposed a robust secure design of beamforming at a SBS and an RIS to maximize the worst-case SR of SUs in [5]. Moreover, the work in [16] also considered enhancing the SR of SUs subject to the total power constraint of SBS and interference power constraint at PUs. In this context, the authors considered three CSI cases for Eve, namely, full, imperfect and no CSI, where they jointly designed beamformers at the SBS and the RIS phase shifts.

It is worth mentioning that [5] and [16] focused on the SR performance without considering the mutual interference between the primary and secondary networks. Motivated by this observation, the authors of [17] proposed a joint beamforming scheme between the primary base station (PBS) and the SBS to enhance the secure operation of the primary network by exploiting the interference of the secondary network while ensuring the SUs communication quality of service (QoS). Accordingly, the authors formulated a total power minimization problem taking into account the OoS of the SUs and the SR requirement of the PUs in order to design the transmit and RIS beamformers alternatively. The work in [18] optimizes the trajectory of a rotary-wing UAV jammer and power allocation to maximize secure energy efficiency in a relay-assisted millimeter wave cognitive radio system. Using an approximate propagation model, the ergodic rate bounds for communication links are derived. The study then establishes an optimal UAV trajectory and resource allocation framework considering interference, information-causality, and UAV propulsion energy constraints. The work [19] evaluates the physical layer security of NOMA-enabled overlay cognitive radio networks in the presence of a passive eavesdropper. Authors have derived secrecy outage probabilities (SOPs) for both primary and secondary users in a jamming-free environment and propose a jammingassisted framework with full-duplex destination nodes to improve PLS. The jamming-assisted approach significantly reduces SOPs and optimal power allocation coefficients are determined to maximize secrecy throughput.

# **III. SYSTEM MODEL**

As shown in Fig. 1, this paper investigates the secure operation of an RIS-assisted CR system, wherein the secondary

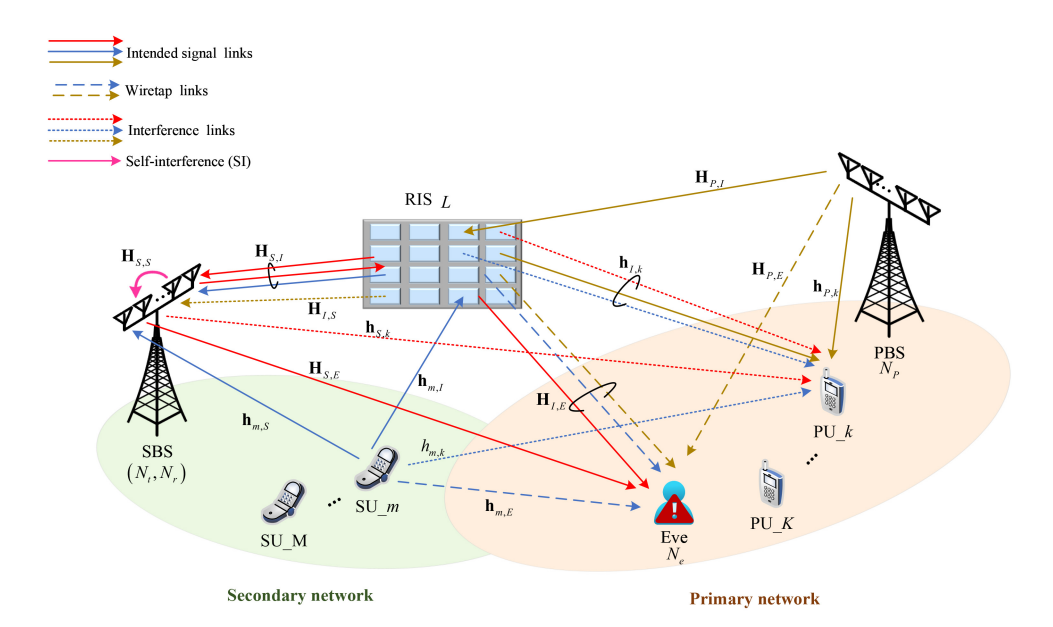


FIGURE 1. An RIS-aided secure CR system.

network shares the same spectrum with the primary one in an underlay fashion. The PBS is assumed to be equipped with  $N_p$  antennas and to send confidential signals to K single-antenna PUs. In the secondary network, a FD-SBS dedicates  $N_r$  receiving antennas to provide an UL service for M single-antenna SUs and meanwhile, directs an AJ signal via  $N_t$  transmitting antennas to prevent a potential Eve, with  $N_e$  antennas, from intercepting the PBS signals. An RIS with L reflecting elements is also used to enhance the SR performance of the CR system. The corresponding sets of PUs, SUs and RIS elements are, respectively, given

by  $K = \{1, ..., K\}$ ,  $M = \{1, ..., M\}$ , and  $L = \{1, ..., L\}$ . Moreover, we assume that the direct links follow Rayleigh fading [22], [23] while the RIS-aided channels follow a Rician fading model [24].

# 1) PRIMARY DL SIGNALING

Assuming that the PBS transmits a signal  $x_k$ ,  $\mathbb{E}\{|x_k|^2\}$  = 1, for each PU  $k \in \mathcal{K}$ . Then, the received signal at user k is given by (1a), on bottom of the page. In (1a),  $P_m$  represents the UL transmission power of the  $m^{\text{th}}$  SU, which

$$y_{k} = \underbrace{\left(\boldsymbol{h}_{P,k}^{H} + \boldsymbol{h}_{I,k}^{H}\boldsymbol{\Theta}\boldsymbol{H}_{P,I}\right)\boldsymbol{v}_{k}x_{k}}_{\text{signals from PBS}} + \underbrace{\left(\boldsymbol{h}_{P,k}^{H} + \boldsymbol{h}_{I,k}^{H}\boldsymbol{\Theta}\boldsymbol{H}_{P,I}\right)\sum_{k'\neq k}\boldsymbol{v}_{k'}x_{k'}}_{\text{inter-user interference}} + \underbrace{\sum_{m=1}^{M}\sqrt{P_{m}}\left(\boldsymbol{h}_{m,k} + \boldsymbol{h}_{I,k}^{H}\boldsymbol{\Theta}\boldsymbol{h}_{m,I}\right)\boldsymbol{s}_{m}}_{\text{interference from UL}}$$

$$+ \underbrace{\left(\boldsymbol{h}_{S,k}^{H} + \boldsymbol{h}_{I,k}^{H}\boldsymbol{\Theta}\boldsymbol{H}_{S,I}\right)\boldsymbol{w}z}_{\text{AJ interference}} + \boldsymbol{n}_{k}, \tag{1a}$$

$$\mathbf{y}_{E,k} = \underbrace{\left(\mathbf{H}_{P,E}^{H} + \mathbf{H}_{I,E}^{H} \mathbf{\Theta} \mathbf{H}_{P,I}\right) \mathbf{v}_{k} \mathbf{x}_{k}}_{\text{Wiretapped PU}_{k}} + \underbrace{\left(\mathbf{H}_{P,E}^{H} + \mathbf{H}_{I,E}^{H} \mathbf{\Theta} \mathbf{H}_{P,I}\right) \sum_{k' \neq k} \mathbf{v}_{k'} \mathbf{x}_{k'}}_{\text{interference from other PUs}} + \underbrace{\sum_{m=1}^{M} \sqrt{P_{m}} \left(\mathbf{h}_{m,E}^{H} + \mathbf{H}_{I,E}^{H} \mathbf{\Theta} \mathbf{h}_{m,I}\right) \mathbf{s}_{m}}_{\text{interference from UL}} + \underbrace{\left(\mathbf{H}_{S,E}^{H} + \mathbf{H}_{I,E}^{H} \mathbf{\Theta} \mathbf{H}_{S,I}\right) \mathbf{w}_{Z}}_{\text{AJ signal}} + \mathbf{n}_{E}, \tag{1b}$$

$$SINR_{k} = \frac{\left|\bar{\boldsymbol{h}}_{PI,k}\boldsymbol{v}_{k}\right|^{2}}{\sum_{k'\neq k}\left|\bar{\boldsymbol{h}}_{PI,k}\boldsymbol{v}_{k'}\right|^{2} + \sum_{m=1}^{M}P_{m}\left|\bar{h}_{m,I,k}\right|^{2} + \left|\bar{\boldsymbol{h}}_{SI,k}\boldsymbol{w}\right|^{2} + \sigma_{k}^{2}},$$
(1c)

$$SINR_{E,k} = \frac{\left|\boldsymbol{\omega}_{E}^{H} \bar{\boldsymbol{H}}_{PIE} \boldsymbol{v}_{k}\right|^{2}}{\sum_{k' \neq k} \left|\boldsymbol{\omega}_{E}^{H} \bar{\boldsymbol{H}}_{PIE} \boldsymbol{v}_{k'}\right|^{2} + \sum_{m=1}^{M} P_{m} \left|\boldsymbol{\omega}_{E}^{H} \bar{\boldsymbol{h}}_{m,IE}\right|^{2} + \left|\boldsymbol{\omega}_{E}^{H} \bar{\boldsymbol{H}}_{SIE} \boldsymbol{w}\right|^{2} + \sigma_{E}^{2} \left\|\boldsymbol{\omega}_{E}^{H}\right\|^{2}},$$
(1d)

transmits the signal  $s_m$ ,  $\mathbb{E}\{|s_m|^2\}=1$  and the signal z,  $\mathbb{E}\{|z|^2\}=1$  refers to the AJ signal. We denote the AJ and PBS beamformers for PU k by  $\mathbf{w} \in \mathbb{C}^{N_t \times 1}$  and  $\mathbf{v}_k \in \mathbb{C}^{N_P \times 1}$ , where the upper limit on AJ and PBS transmission powers,  $P_z^{\text{max}}$  and  $P_{DL}^{\text{max}}$ , respectively, should be guaranteed by setting  $\operatorname{Tr}(\boldsymbol{W}) \leq P_z^{\max}$  and  $\sum_{k=1}^K \operatorname{Tr}(\boldsymbol{V}_k) \leq P_{DL}^{\max}$ , where  $\boldsymbol{W} = \boldsymbol{w}\boldsymbol{w}^H$  and  $\boldsymbol{V}_k = \boldsymbol{v}_k \boldsymbol{v}_k^H$ . Also,  $n_k$  denotes the additive white Gaussian noise (AWGN) with zero mean and variance  $\sigma_k^2$ , i.e.,  $n_k \sim$  $\mathcal{CN}(0, \sigma_k^2)$ . Similar to (1a), the received signal at Eve when tapping into PU k's signal is expressed as in (1b), also on bottom of the previous page, where  $\mathbf{n}_E \sim \mathcal{CN}(0, \sigma_F^2 \mathbf{I}_{N_e})$ denotes the AWGN.

Furthermore, in the above equations, the RIS reflection coefficient matrix is defined by  $\Theta$  $\operatorname{diag}(a_1e^{j\varphi_1},\ldots,a_Le^{j\varphi_L})\in\mathbb{C}^{L\times L}$ , where  $a_l$  and  $\varphi_l$  express the amplitude and phase shift responses of the element l. We assume that the RIS performs maximum reflection without losses for the incident signal, i.e.,  $a_l = 1$ , accordingly the RIS phase shift matrix is denoted as  $\Theta = \operatorname{diag}(\theta)$  where  $\boldsymbol{\theta} = [e^{j\varphi_1}, \dots, e^{j\varphi_L}]^T$ ,  $\theta_l = e^{j\varphi_l}$  and  $\varphi_l \in [0, 2\pi)$ ,  $\forall l \in \mathcal{L}$ .

In addition, the channels  $\mathbf{h}_{P,k} \in \mathbb{C}^{N_P \times 1}, \mathbf{h}_{I,k} \in \mathbb{C}^{L \times 1}$ and  $\mathbf{H}_{P,I} \in \mathbb{C}^{L \times N_P}$  denote the PBS-PU k, RIS-PU k and PBS-RIS baseband channels, respectively. Moreover, the channels from the m-th SU to PU k and the RIS are given by  $h_{m,k}$  and  $\mathbf{h}_{m,l} \in \mathbb{C}^{L \times 1}$ , respectively. The jamming interference channels from the SBS to PU k and the RIS are denoted by  $\mathbf{h}_{S,k} \in \mathbb{C}^{N_t \times 1}$  and  $\mathbf{H}_{S,L} \in \mathbb{C}^{L \times N_t}$ . The eavesdropping channels, denoted by  $\mathbf{H}_{P,E} \in \mathbb{C}^{N_P \times N_e}$  and  $\mathbf{H}_{I,E} \in \mathbb{C}^{L \times N_e}$ , represent the PBS-Eve and the RIS-Eve channels, respectively. Finally,  $\mathbf{h}_{m,E} \in \mathbb{C}^{1 \times N_e}$  and  $\mathbf{H}_{S,E} \in$  $\mathbb{C}^{N_t \times N_e}$  denote the channels from Eve to SU *m* and the SBS, respectively.

For notation simplicity, we define the cascaded and direct channel links in (1a) and (1b) as  $\bar{h}_{PI,k} = h_{Pk}^H + h_{Ik}^H \Theta H_{P,I}$ ,  $\bar{h}_{m,I,k} = h_{m,k} + h_{I,k}^H \Theta h_{m,I}, \ \bar{h}_{SI,k} = h_{S,k}^H + h_{I,k}^H \Theta H_{S,I}$  and  $\bar{H}_{PIE} = H_{P,E}^H + H_{I,E}^H \Theta H_{P,I}, \ \bar{h}_{m,IE} = h_{m,E}^H + H_{I,E}^H \Theta h_{m,I},$   $\bar{H}_{SIE} = H_{S,E}^H + H_{I,E}^H \Theta H_{S,I}.$  In this analysis, we assume the legitimate side has complete knowledge of the channel state information (CSI), including details on both reflection and wiretap links. The assumption of perfect CSI at the BS serves as a theoretical simplification to streamline our analysis, yet it may not precisely reflect the intricacies of real-world conditions. We recognize the importance of studying robust design by considering imperfect cascaded

CSI, as in [25], [26], [27], [28]. However, as is common in the literature, e.g., references [2], [12], [17], [19], the focus of our current work is to introduce and optimize one complex system integrated with multiple technologies, including FD communication, cognitive radio, a physical layer security mechanism, and RIS. We intentionally included perfect CSI to control the scope and complexity of this initial study. Addressing imperfect CSI requires remodeling, sophisticated analysis and would significantly extend the scope of our current work. A typical example fitting these assumptions is the uplink transmission scenario, where a full-duplex base station communicates with the intended transmitter while jamming an unscheduled user. Therefore, the eavesdropper can only adjust its receive beamforming based on the wiretap channel information.

The received signal-to-interference-plus-noise ratio (SINR) at PU k and Eve when tapping into PU k are, respectively, given by (1c) and (1d), on bottom of the previous page, where Eve deploys receive beamformers  $\boldsymbol{\omega}_E \in \mathbb{C}^{N_e \times 1}$  such that the achievable SINR at Eve, in (1d), is evaluated after post-processing via  $\boldsymbol{\omega}_{F}^{H} \mathbf{y}_{E,k}$ . We assume that Eve can determine its receive beamforming  $\omega_E$  based on the direct wiretap channel. Specifically, Eve computes the singular value decomposition (SVD) of the channel matrix  $H_{P,E}$  as  $H_{P,E} = \mathbf{A} \mathbf{\Sigma} \mathbf{B}^H$ , where **A** and **B** are unitary matrices and  $\Sigma$  is a diagonal matrix containing the singular values of  $H_{PF}^H$ . Then, the receive beamforming vector, according to maximum ratio combining (MRC), can be chosen as the right singular vector corresponding to the largest singular value of the channel matrix, at which Eve tries to maximize its achievable rate, i.e.,  $\boldsymbol{\omega}_E = \boldsymbol{B}(:,1)$ . Accordingly, the achievable secrecy rate at PU k can be calculated as  $SR_k =$  $\max_{k} \{ \log_2(1 + SINR_k) - \log_2(1 + SINR_{E,k}), 0 \}.$ 

# 2) SECONDARY UL SIGNALING

Cognitive Radio (CR) technology facilitates the coexistence of primary and secondary networks by allowing them to share the spectrum, thereby improving spectral efficiency. Nonetheless, the risk of interception by eavesdroppers, particularly those equipped with multiple antennas, remains a concern. This raises a critical question: how do we maximize the advantages of both spectrum sharing and security

<sup>1</sup>Similar applications include Internet of Things (IoT) communications and unmanned aerial vehicle (UAV) communications.

$$\mathbf{y}_{B} = \underbrace{\sum_{m=1}^{m} \sqrt{P_{m}} \left(\mathbf{h}_{m,S}^{H} + \mathbf{H}_{I,S}^{H} \mathbf{\Theta} \mathbf{h}_{m,I}\right) s_{m}}_{\text{UL signals}} + \underbrace{\left(\mathbf{H}_{P,S}^{H} + \mathbf{H}_{I,S}^{H} \mathbf{\Theta} \mathbf{H}_{P,I}\right) \sum_{k=1}^{K} \mathbf{v}_{k} x_{k}}_{\text{PUs signal}} + \underbrace{\left(\sqrt{\delta} \mathbf{H}_{S,S}^{H} + \mathbf{H}_{I,S}^{H} \mathbf{\Theta} \mathbf{H}_{S,I}\right) \mathbf{w}_{Z}}_{\text{AJ self-interference}} + \mathbf{n}_{B}, \quad (2a)$$

$$SINR_{m} = \frac{P_{m} \left|\mathbf{\omega}_{B,m}^{H} \bar{\mathbf{h}}_{m,IS}\right|^{2}}{\sum_{m' \neq m} P_{m'} \left|\mathbf{\omega}_{B,m}^{H} \bar{\mathbf{h}}_{m',IS}\right|^{2} + \sum_{k=1}^{K} \left|\mathbf{\omega}_{B,m}^{H} \bar{\mathbf{H}}_{PIS} \mathbf{v}_{k}\right|^{2} + \left|\mathbf{\omega}_{B,m}^{H} \bar{\mathbf{H}}_{SIS} \mathbf{w}\right|^{2} + \sigma_{B}^{2} \left\|\mathbf{\omega}_{B,m}^{H}\right\|^{2}}. \quad (2b)$$

$$SINR_{m} = \frac{P_{m} \left| \boldsymbol{\omega}_{B,m}^{H} \bar{\boldsymbol{h}}_{m,IS} \right|^{2}}{\sum_{m' \neq m} P_{m'} \left| \boldsymbol{\omega}_{B,m}^{H} \bar{\boldsymbol{h}}_{m',IS} \right|^{2} + \sum_{k=1}^{K} \left| \boldsymbol{\omega}_{B,m}^{H} \bar{\boldsymbol{H}}_{PIS} \boldsymbol{v}_{k} \right|^{2} + \left| \boldsymbol{\omega}_{B,m}^{H} \bar{\boldsymbol{H}}_{SIS} \boldsymbol{w} \right|^{2} + \sigma_{B}^{2} \left\| \boldsymbol{\omega}_{B,m}^{H} \right\|^{2}}.$$
(2b)

without compromising either? To answer this question, our paper aims to enhance the PLS of RIS-assisted CR networks by exploiting the secondary network. Specifically, the dual functionality of the FD-SBS not only strengthens the PLS through flexible and actively performing jamming capabilities but also ensures that the QoS of the secondary network will be guaranteed with reduced interference toward the primary network. The received signal  $\mathbf{y}_R \in \mathbb{C}^{N_r \times 1}$  at the SBS includes the UL signals from the M SUs and the DL of the PBS as well as the self-interference from the AJ signal. Hence,  $y_B$  can be expressed as in (2a), on bottom of the previous page, where  $\mathbf{n}_B \sim \mathcal{CN}(0, \sigma_B^2 \mathbf{I}_{N_r})$ . Similar to the previous subsection, the direct and cascaded UL channels are simplified as  $\bar{\boldsymbol{h}}_{m,IS} = \boldsymbol{h}_{m,S}^H + \boldsymbol{H}_{I,S}^H \boldsymbol{\Theta} \boldsymbol{h}_{m,I}, \, \bar{\boldsymbol{H}}_{PIS} = \boldsymbol{H}_{P,S}^H + \boldsymbol{H}_{I,S}^H \boldsymbol{\Theta} \boldsymbol{H}_{P,I}, \, \bar{\boldsymbol{H}}_{SIS} = \sqrt{\delta} \boldsymbol{H}_{S,S}^H + \boldsymbol{H}_{I,S}^H \boldsymbol{\Theta} \boldsymbol{H}_{S,I}, \, \text{ where } \boldsymbol{H}_{S,S}$  is the self-interference channel with suppression ratio  $\delta$ . By defining  $\boldsymbol{\omega}_{B,m} \in \mathbb{C}^{N_r \times 1}$  as the receive beamforming at the SBS for the m-th UL signal and processing it via multiplying (2a) by  $\omega_{B,m}^H$ , the received m-th user SINR at the SBS is expressed as in (2b), also on bottom of the previous page. Finally, the corresponding achievable UL rate is  $R_m = \log_2(1 + SINR_m)$ .

# IV. OPTIMIZATION PROBLEM FORMULATION

As mentioned earlier, in this section, we aim at maximizing the minimum (worst-case) secrecy rate of the PUs by jointly optimizing the PBS beamformers  $\{v_k\}$ , the AJ beamforming vectors  $\boldsymbol{w}$ , the FD-SBS receive beamformers  $\{\boldsymbol{\omega}_{B,m}\}$ , the UL power  $\{P_m\}$  as well as the RIS<sup>2</sup> reflection coefficient matrix  $\boldsymbol{\Theta}$ . This needs to be done while ensuring minimum QoS requirements for the SUs along with respecting the allowed power budget of the PBS and receive and AJ beamformers' requirements. Therefore, the main problem can be formulated as

$$\begin{array}{c}
\text{Maximize } \text{Min } SR_k \\
\mathbf{V}_k, \mathbf{W}, \boldsymbol{\omega}_{B,m}, \mathbf{\Theta}, P_m \quad k
\end{array} \tag{3a}$$

subject to:

$$\log_2(1 + SINR_m) \ge R_{UL}^{th}, \forall m \in \mathcal{M}, \tag{3b}$$

$$\|\boldsymbol{\omega}_{B,m}\|^2 = 1, \forall m \in \mathcal{M},$$
 (3c)

$$Tr(\boldsymbol{W}) < P_{z}^{\max}, \tag{3d}$$

<sup>2</sup>In case of active RIS, we can follow the adopted framework to reformulate (3) by considering additional noise term imposed by active amplification. Further, the unit-modulus constraint should be replaced by power budget and amplification coefficients at active RIS [29], [30]. However, these additional terms and constraints will further restrict the problem feasibility.

$$\sum_{k=1}^{K} \operatorname{Tr}(\boldsymbol{V}_k) \le P_{DL}^{\max}, \tag{3e}$$

$$P_m \le P_m^{\text{max}}, \forall m \in \mathcal{M},$$
 (3f)

$$\varphi_l \in [0, 2\pi), \forall l \in \mathcal{L},$$
(3g)

where constraint (3b) ensures a minimum rate  $R_{III}^{th}$  for each SU  $m \in \mathcal{M}$  and constraint (3c) represents the normalization condition for the SBS receive beamforming. The downlink power budget for AJ and the PUs beamforming are represented in (3d) and (3e), respectively. Also, the UL power budget for the SUs is ensured by (3f). Finally, the unit-modulus constraint of the RIS is captured by (3g). Clearly, the problem in (3) is non-convex due to the coupling between the optimization variables in the objective and the constraints. To solve this issue, we first reformulate the objective  $SR_k$  into a tractable upper bound. Then, we adopt an AO method to divide the original problem (3) into four sub-problems, namely, optimizing the jamming beamforming matrix at the FD-SBS, the UL transmit power of the SUs, the DL beamformers at the PBS and finally, the UL receive beamforming and RIS passive beamformers, throughout which the optimization variables are independently decoupled and solved using SDP and SCA. These sub-problems are discussed in the following subsections.

# A. UL RECEIVE BEAMFORMING VECTORS ( $\omega_{B,M}$ )

To find the optimal receive beamforming vectors with fixed other variables  $\{v_k\}$ , w,  $\{P_m\}$  and  $\Theta$ , the optimization problem (3) can be rewritten as

$$\begin{array}{ll}
\text{Maximize SINR}_m & (4a)
\end{array}$$

subject to: 
$$\|\boldsymbol{\omega}_{B,m}\|^2 = 1, \forall m \in \mathcal{M},$$
 (4b)

where problem (4) can be regarded as a generalized eigenvalue problem [31]. Therefore, the optimum solution of  $\omega_{B,m}$  can be evaluated as in (5), on bottom of the page.

# B. JOINT BEAMFORMING OF PBS AND AJ ( $V_K$ , W)

We consider designing the beamforming of the PBS for all the PUs and AJ as well, given that the variables  $\omega_B$ ,  $\{P_m\}$  and  $\Theta$  are all fixed. The optimization problem (3) can be expressed as

$$\text{Maximize } \min_{\boldsymbol{V}_k, \boldsymbol{W}} SR_k \tag{6a}$$

subject to

$$\log_2(1 + SINR_m) \ge R_{UL}^{th}, \forall m \in \mathcal{M}, \tag{6b}$$

$$Tr(\mathbf{W}) \le P_{\tau}^{\max},\tag{6c}$$

$$\boldsymbol{\omega}_{B,m} = \frac{\left(\sum_{m' \neq m} P_{m'} \bar{\boldsymbol{h}}_{m',IS} \bar{\boldsymbol{h}}_{m',IS}^{H} + \sum_{k=1}^{K} \bar{\boldsymbol{H}}_{PIS} \boldsymbol{V}_{k} \bar{\boldsymbol{H}}_{PIS}^{H} + \bar{\boldsymbol{H}}_{SIS} \boldsymbol{W} \bar{\boldsymbol{H}}_{SIS}^{H} + \sigma_{B}^{2} \boldsymbol{I}_{N_{r}}\right)^{-1} \bar{\boldsymbol{h}}_{m,IB}}{\left\|\left(\sum_{m' \neq m} P_{m'} \bar{\boldsymbol{h}}_{m',IS} \bar{\boldsymbol{h}}_{m',IS}^{H} + \sum_{k=1}^{K} \bar{\boldsymbol{H}}_{PIS} \boldsymbol{V}_{k} \bar{\boldsymbol{H}}_{PIS}^{H} + \bar{\boldsymbol{H}}_{SIS} \boldsymbol{W} \bar{\boldsymbol{H}}_{SIS}^{H} + \sigma_{B}^{2} \boldsymbol{I}_{N_{r}}\right)^{-1} \bar{\boldsymbol{h}}_{m,IB}}\right\|, \forall m \in \mathcal{M}.$$
(5)

$$\sum_{k=1}^{K} \operatorname{Tr}(\boldsymbol{V}_k) \le P_{DL}^{\max}. \tag{6d}$$

However, problem (6) is non-convex in  $V_k$  and W. To address this issue, we first note that the signal and SUs interference terms of SINR<sub>k</sub>, in (1c), can be re-expressed as

$$\begin{aligned} \left| \bar{\boldsymbol{h}}_{PI,k} \boldsymbol{v}_{k} \right|^{2} &= \bar{\boldsymbol{h}}_{PI,k} \boldsymbol{V}_{k} \bar{\boldsymbol{h}}_{PI,k}^{H} = \operatorname{Tr}(\bar{\boldsymbol{H}}_{PI,k} \boldsymbol{V}_{k}) \\ \left| \bar{\boldsymbol{h}}_{SI,k} \boldsymbol{w} \right|^{2} &= \bar{\boldsymbol{h}}_{SI,k} \boldsymbol{W} \bar{\boldsymbol{h}}_{SI,k}^{H} = \operatorname{Tr}(\bar{\boldsymbol{H}}_{SI,k} \boldsymbol{W}), \end{aligned}$$

where  $\bar{\boldsymbol{H}}_{PI,k} = \bar{\boldsymbol{h}}_{PI,k}^H \bar{\boldsymbol{h}}_{PI,k} \in \mathbb{C}^{N_P \times N_P}$  and  $\bar{\boldsymbol{H}}_{SI,k} = \bar{\boldsymbol{h}}_{SI,k}^H \bar{\boldsymbol{h}}_{SI,k} \in \mathbb{C}^{N_t \times N_t}$ . Similarly, the numerator of SINR<sub>E,k</sub> in (1d) can be re-written as

$$\left| \boldsymbol{\omega}_{E}^{H} \bar{\boldsymbol{H}}_{PIE} \boldsymbol{v}_{k} \right|^{2} = \boldsymbol{\omega}_{E}^{H} \bar{\boldsymbol{H}}_{PIE} \boldsymbol{V}_{k} \bar{\boldsymbol{H}}_{PIE}^{H} \boldsymbol{\omega}_{E} = \widehat{\boldsymbol{h}}_{PIE} \boldsymbol{V}_{k} \widehat{\boldsymbol{h}}_{PIE}^{H}$$
$$= \operatorname{Tr}(\widehat{\boldsymbol{H}}_{PIE} \boldsymbol{V}_{k})$$

where  $\widehat{\mathbf{h}}_{PIE} = \boldsymbol{\omega}_E^H \overline{\mathbf{h}}_{PIE} \in \mathbb{C}^{1 \times N_P}$  and  $\widehat{\mathbf{H}}_{PIE} = \widehat{\mathbf{h}}_{PIE}^H \widehat{\mathbf{h}}_{PIE} \in \mathbb{C}^{N_P \times N_P}$ . Moreover, in the denominator, we have

$$\left| \boldsymbol{\omega}_{E}^{H} \boldsymbol{\bar{H}}_{SIE} \boldsymbol{w} \right|^{2} = \boldsymbol{\omega}_{E}^{H} \boldsymbol{\bar{H}}_{SIE} \boldsymbol{W} \boldsymbol{\bar{H}}_{SIE}^{H} \boldsymbol{\omega}_{E}$$
$$= \hat{\boldsymbol{h}}_{SIE} \boldsymbol{W} \hat{\boldsymbol{h}}_{SIE}^{H} = \text{Tr}(\hat{\boldsymbol{H}}_{SIE} \boldsymbol{W})$$

where  $\hat{\boldsymbol{h}}_{SIE} = \boldsymbol{\omega}_E^H \bar{\boldsymbol{h}}_{SIE} \in \mathbb{C}^{1 \times N_t}$  and  $\hat{\boldsymbol{H}}_{SIE} = \hat{\boldsymbol{h}}_{SIE}^H \hat{\boldsymbol{h}}_{SIE} \in \mathbb{C}^{N_t \times N_t}$ . Accordingly, using the above substitutions, the SR in (6a) can be re-expressed as  $\widehat{SR}_k$  in (7), on bottom of the page, where  $I_k = \sum_{m=1}^M P_m |\bar{\boldsymbol{h}}_{m,I,k}|^2 + \sigma_k^2$  and  $I_E = \boldsymbol{\omega}_E^H \sum_{m=1}^M P_m \bar{\boldsymbol{h}}_{m,IE} \hat{\boldsymbol{h}}_{m,IE}^H \boldsymbol{\omega}_E + \sigma_E^2 \boldsymbol{\omega}_E^H \boldsymbol{I}_{N_e} \boldsymbol{\omega}_E$ . SR<sub>k</sub> is still non-convex. Therefore, we derive an

 $\widehat{SR}_k$  is still non-convex. Therefore, we derive an upper bound by introducing the auxiliary variables  $p_k = [p_{1,k}, p_{2,k}, p_{3,k}, p_{4,k}]^T$  into the objective, such that the achievable rate at PU k and Eve are bounded as  $R_k \ge p_{1,k} - p_{2,k}$  and  $R_{E,k} \le p_{3,k} - p_{4,k}$ , respectively. Hence, the achievable rates  $R_k$  and  $R_{E,k}$  should satisfy the following constraints:

$$R_{k} \Leftrightarrow \begin{cases} \log_{2}\left(\operatorname{Tr}(\bar{\boldsymbol{H}}_{PI,k}\boldsymbol{V}_{k}) + \sum_{k' \neq k} \operatorname{Tr}(\bar{\boldsymbol{H}}_{PI,k}\boldsymbol{V}_{k'}) \right. \\ + \operatorname{Tr}(\bar{\boldsymbol{H}}_{SI,k}\boldsymbol{W}) + I_{k}\right) \geq p_{1,k}, \\ \log_{2}\left(\sum_{k' \neq k} \operatorname{Tr}(\bar{\boldsymbol{H}}_{PI,k}\boldsymbol{V}_{k'}) + \operatorname{Tr}(\bar{\boldsymbol{H}}_{SI,k}\boldsymbol{W}) \right. \\ + I_{k}\right) \leq p_{2,k}, \end{cases}$$
(8)

$$R_{E,k} \Leftrightarrow \begin{cases} \log_2 \left( \operatorname{Tr}(\widehat{\boldsymbol{H}}_{PIE} \boldsymbol{V}_k) + \sum_{k' \neq k} \operatorname{Tr}(\widehat{\boldsymbol{H}}_{PIE} \boldsymbol{V}_{k'}) \right) \\ + \operatorname{Tr}(\widehat{\boldsymbol{H}}_{SIE} \boldsymbol{W}) + I_E \right) \leq p_{3,k}, \\ \log_2 \left( \sum_{k' \neq k} \operatorname{Tr}(\widehat{\boldsymbol{H}}_{PIE} \boldsymbol{V}_{k'}) + \operatorname{Tr}(\widehat{\boldsymbol{H}}_{SIE} \boldsymbol{W}) \right) \\ + I_E \right) \geq p_{4,k}. \end{cases}$$
(9)

In addition, noting that

$$\boldsymbol{\omega}_{B,m}^{H} \sum_{k=1}^{K} \bar{\boldsymbol{H}}_{PIS} \boldsymbol{V}_{k} \bar{\boldsymbol{H}}_{PIS}^{H} \boldsymbol{\omega}_{B,m} = \sum_{k=1}^{K} \operatorname{Tr}(\widehat{\boldsymbol{H}}_{PIS} \boldsymbol{V}_{k}),$$
$$\boldsymbol{\omega}_{B,m}^{H} \bar{\boldsymbol{H}}_{SIS} \boldsymbol{W} \bar{\boldsymbol{H}}_{SIS}^{H} \boldsymbol{\omega}_{B,m} = \widehat{\boldsymbol{h}}_{SIS} \boldsymbol{W} \widehat{\boldsymbol{h}}_{SIS}^{H} = \operatorname{Tr}(\widehat{\boldsymbol{H}}_{SIS} \boldsymbol{W}),$$

the achievable UL rate for the  $m^{th}$  SU can be represented in terms of active beamforming as

$$\widetilde{R_m} = \log_2 \left( 1 + \frac{\widetilde{s}_m}{I_m + \sum_{k=1}^K \text{Tr}(\widehat{\boldsymbol{H}}_{PIS} \boldsymbol{V}_k) + \text{Tr}(\widehat{\boldsymbol{H}}_{SIS} \boldsymbol{W})} \right), \tag{10}$$

where  $\tilde{s}_m = P_m \boldsymbol{\omega}_{B,m}^H \bar{\boldsymbol{h}}_{m,IS} \bar{\boldsymbol{h}}_{m,IS}^H \boldsymbol{\omega}_{B,m}$  and  $I_m = \boldsymbol{\omega}_{B,m}^H \sum_{m' \neq m} P_{m'} \bar{\boldsymbol{h}}_{m',IS} \bar{\boldsymbol{h}}_{m',IS}^H \boldsymbol{\omega}_{B,m} + \sigma_B^2 \boldsymbol{\omega}_{B,m}^H \boldsymbol{I}_{N_t} \boldsymbol{\omega}_{B,m}$  with  $\widehat{\boldsymbol{H}}_{PIS} = \widehat{\boldsymbol{h}}_{PIS}^H \widehat{\boldsymbol{h}}_{PIS}$ ,  $\widehat{\boldsymbol{h}}_{PIS} = \boldsymbol{\omega}_B^H \bar{\boldsymbol{H}}_{PIS}$ ,  $\widehat{\boldsymbol{h}}_{SIS} = \boldsymbol{\omega}_B^H \bar{\boldsymbol{H}}_{SIS} \in \mathbb{C}^{1 \times N_t}$  and  $\widehat{\boldsymbol{H}}_{SIS} = \widehat{\boldsymbol{h}}_{SIS}^H \widehat{\boldsymbol{h}}_{SIS} \in \mathbb{C}^{N_t \times N_t}$ . Hence, the current optimization sub problem is given by

Maximize 
$$\min_{\mathbf{V}_k, \mathbf{W}} \min_{k} p_{1,k} - p_{2,k} - p_{3,k} + p_{4,k}$$
 (11a)

subject to:

$$\widetilde{R_m} \ge R_{UL}^{\text{th}}, \, \forall m \in \mathcal{M},$$
 (11c)

$$\sum_{k=1}^{K} \operatorname{Tr}(\boldsymbol{V}_k) \le P_{DL}^{\max}, \quad \operatorname{Tr}(\boldsymbol{W}) \le P_{z}^{\max}, (11d)$$

$$\mathbf{W} \geq 0, \mathbf{V}_k \geq 0,$$
 (11e)

$$Rank(\mathbf{W}) = Rank(\mathbf{V}_k) = 1. \tag{11f}$$

However, problem (11) is an SDP and is still non-convex due to the non-convex constraints (11b) and (11f). Moreover, the inequalities in (11b) hold at the optimum solution, so that the problem (11) is equivalent to (6). Dealing with the non-convexity of constraint (11b), we introduce additional

$$\widetilde{SR}_{k}(\boldsymbol{V}_{k}, \boldsymbol{W}) = \log_{2} \left( \frac{\operatorname{Tr}(\bar{\boldsymbol{H}}_{PI,k}\boldsymbol{V}_{k}) + \sum_{k' \neq k} \operatorname{Tr}(\bar{\boldsymbol{H}}_{PI,k}\boldsymbol{V}_{k'}) + \operatorname{Tr}(\bar{\boldsymbol{H}}_{SI,k}\boldsymbol{W}) + I_{k}}{\sum_{k' \neq k} \operatorname{Tr}(\bar{\boldsymbol{H}}_{PI,k}\boldsymbol{V}_{k'}) + \operatorname{Tr}(\bar{\boldsymbol{H}}_{SI,k}\boldsymbol{W}) + I_{k}} \right) - \log_{2} \left( \frac{\operatorname{Tr}(\widehat{\boldsymbol{H}}_{PIE}\boldsymbol{V}_{k}) + \sum_{k' \neq k} \operatorname{Tr}(\widehat{\boldsymbol{H}}_{PIE}\boldsymbol{V}_{k'}) + \operatorname{Tr}(\widehat{\boldsymbol{H}}_{SIE}\boldsymbol{W}) + I_{E}}{\sum_{k' \neq k} \operatorname{Tr}(\widehat{\boldsymbol{H}}_{PIE}\boldsymbol{V}_{k'}) + \operatorname{Tr}(\widehat{\boldsymbol{H}}_{SIE}\boldsymbol{W}) + I_{E}} \right).$$
(7)

auxiliary variables  $\Omega_r = \{r_{1,k}, r_{2,k}, r_{3,k}, r_{4,k}\}$  into (7). Hence, the objective recast as

$$\widetilde{R}_{k} \Leftrightarrow \begin{cases} \log_{2}(r_{1,k}) \geq p_{1,k}, & (12a) \\ \operatorname{Tr}(\widetilde{\boldsymbol{H}}_{PI,k}\boldsymbol{V}_{k}) + \sum_{k' \neq k} \operatorname{Tr}(\widetilde{\boldsymbol{H}}_{PI,k}\boldsymbol{V}_{k'}) & \\ + \operatorname{Tr}(\widetilde{\boldsymbol{H}}_{SI,k}\boldsymbol{W}) + I_{k} \geq r_{1,k}, & (12b) \\ \log_{2}(r_{2,k}) \leq p_{2,k}, & (12c) \\ \sum_{k' \neq k} \operatorname{Tr}(\widetilde{\boldsymbol{H}}_{PI,k}\boldsymbol{V}_{k'}) + \operatorname{Tr}(\widetilde{\boldsymbol{H}}_{SI,k}\boldsymbol{W}) & \\ + I_{k} \leq r_{2,k}, & (12d) \end{cases}$$

and

$$\widetilde{R_{E,k}} \Leftrightarrow \begin{cases}
\log_2(r_{3,k}) \leq p_{3,k}, & (13a) \\
\operatorname{Tr}(\widehat{\boldsymbol{H}}_{PIE}\boldsymbol{V}_k) + \sum_{k' \neq k} \operatorname{Tr}(\widehat{\boldsymbol{H}}_{PIE}\boldsymbol{V}_{k'}) & \\
+ \operatorname{Tr}(\widehat{\boldsymbol{H}}_{SIE}\boldsymbol{W}) + I_E \leq r_{3,k}, & (13b) \\
\log_2(r_{4,k}) \geq p_{4,k}, & (13c) \\
\sum_{k' \neq k} \operatorname{Tr}(\widehat{\boldsymbol{H}}_{PIE}\boldsymbol{V}_{k'}) + \operatorname{Tr}(\widehat{\boldsymbol{H}}_{SIE}\boldsymbol{W}) & \\
+ I_E \geq r_{4,k} \forall k. & (13d)
\end{cases}$$

However, constraints (12c) and (13a) are still non-convex. By invoking the SCA method, these constraints could be handled via first order Taylor approximation at feasible points  $\{\tilde{r}_{2,k}^{(t)}\}$ and  $\{\tilde{r}_{3k}^{(t)}\}$  at the  $t^{\text{th}}$  iteration of an iterative algorithm as follows

$$\log_2(r_{2,k}) \le p_{2,k} \Rightarrow \log_2(\tilde{r}_{2,k}^{(t)}) + \frac{\left(r_{2,k} - \tilde{r}_{2,k}^{(t)}\right)}{\tilde{r}_{2,k}^{(t)} \ln(2)} \le p_{2,k}, (14)$$

$$\log_{2}(r_{2,k}) \leq p_{2,k} \Rightarrow \log_{2}(r_{2,k}^{(r)}) + \frac{\langle r_{2,k}^{(t)} | r_{2,k}^{(t)} \rangle}{\tilde{r}_{2,k}^{(t)} | r_{2,k}^{(t)} \rangle} \leq p_{2,k}, \quad (14)$$

$$\text{where } D_{m} = \sum_{k=1}^{K} |\boldsymbol{\omega}_{B,m}^{H} \bar{\mathbf{H}}_{PIS} \mathbf{v}_{k}|^{2} + |\boldsymbol{\omega}_{B,m}^{H} \bar{\mathbf{H}}_{SIS} \mathbf{w}|^{2} + \sigma_{B}^{2} |\boldsymbol{\omega}_{B,m}^{H}|^{2} \text{ and } \bar{R}_{UL}^{th} = 2^{R_{UL}^{th}} - 1.$$

$$\text{To tackle the non-convexity of the SR in (18), we introduce auxiliary variables } \mathbf{Z}_{k} = [z_{1,k}, z_{2,k}, z_{3,k}, z_{4,k}]^{T}, \text{ which results}$$

respectively. According to the analysis above, the joint PBS beamforming and AJ can finally be expressed as

Maximize 
$$\underset{V_k, \mathbf{W}}{\text{Min }} p_{1,k} - p_{2,k} - p_{3,k} + p_{4,k}$$
 (16a) subject to:

$$\widetilde{s}_{m} - \left(2^{R_{UL}^{\text{th}}} - 1\right) \left(I_{m} + \sum_{k=1}^{K} \text{Tr}(\widehat{\boldsymbol{H}}_{PIS}\boldsymbol{V}_{k})\right) + \text{Tr}(\widehat{\boldsymbol{H}}_{SIS}\boldsymbol{W}) \ge 0,$$
(16c)

$$\sum_{k=1}^{K} \operatorname{Tr}(\boldsymbol{V}_k) \le P_{DL}^{\max}, \quad \operatorname{Tr}(\boldsymbol{W}) \le P_{z}^{\max}, \tag{16d}$$

$$\mathbf{W} \succcurlyeq 0, \mathbf{V}_k \succcurlyeq 0, \tag{16e}$$

which is a relaxed SDP that can be solved using standard convex optimization toolboxes, e.g., CVX [32].

# C. OPTIMIZING THE UL POWER (PM)

Given the optimal variables  $\{v_k\}$ , w,  $\{\omega_{B,m}\}$  and  $\Theta$ , the UL power optimization problem for the SUs can be formulated

$$\underset{P_m}{\text{Maximize Min }} \widetilde{SR}_k(\boldsymbol{V}_k, \boldsymbol{W}) \tag{17a}$$

$$R_m(P_m) \ge R_{UL}^{\text{th}}, \forall m \in \mathcal{M},$$
 (17b)

$$P_m \le P_m^{\max}, \forall m \in \mathcal{M},$$
 (17c)

where the secrecy rate objective is given by

$$\widetilde{SR}_{k}(\mathbf{V}_{k}, \mathbf{W}) = \log_{2} \left( A_{k} + B_{k} + \sum_{m=1}^{M} P_{m} |\bar{h}_{m,I,k}|^{2} \right)$$

$$- \log_{2} \left( B_{k} + \sum_{m=1}^{M} P_{m} |\bar{h}_{m,I,k}|^{2} \right)$$

$$- \log_{2} \left( A_{E,k} + B_{E,k} + \sum_{m=1}^{M} P_{m} |\boldsymbol{\omega}_{E}^{H} \bar{\mathbf{h}}_{m,IE}|^{2} \right)$$

$$+ \log_{2} \left( B_{E,k} + \sum_{m=1}^{M} P_{m} |\boldsymbol{\omega}_{E}^{H} \bar{\mathbf{h}}_{m,IE}|^{2} \right), \quad (18)$$

where  $A_k = \operatorname{Tr}(\bar{\mathbf{H}}_{PI,k}\mathbf{V}_k)$ ,  $B_k = \sum_{k'\neq k}\operatorname{Tr}(\bar{\mathbf{H}}_{PI,k}\mathbf{V}_{k'}) + \operatorname{Tr}(\bar{\mathbf{H}}_{SI,k}\mathbf{W}) + \sigma_k^2$ ,  $A_{E,k} = \operatorname{Tr}(\widehat{\mathbf{H}}_{PIE}\mathbf{V}_k)$  and  $B_{E,k} = \sum_{k'\neq k}\operatorname{Tr}(\widehat{\mathbf{H}}_{PIE}\mathbf{V}_{k'}) + \operatorname{Tr}(\widehat{\mathbf{H}}_{SIE}\mathbf{W}) + \sigma_E^2\|\boldsymbol{\omega}_E^H\|^2$ . Moreover, constraint (17b) can be expressed as

$$\frac{P_{m}\left|\boldsymbol{\omega}_{B,m}^{H}\bar{\mathbf{h}}_{m,IS}\right|^{2}}{\sum_{m'\neq m}P_{m'}\left|\boldsymbol{\omega}_{B,m}^{H}\bar{\mathbf{h}}_{m',IS}\right|^{2}+D_{m}}\geq\bar{R}_{UL}^{th},$$
(19)

auxiliary variables  $\mathbf{Z}_k = [z_{1,k}, z_{2,k}, z_{3,k}, z_{4,k}]^T$ , which results in recasting the objective terms as follows

$$\begin{cases} R_{k} \Leftrightarrow \log_{2}\left(A_{k} + B_{k} + \sum_{m=1}^{M} P_{m} |\bar{h}_{m,l,k}|^{2}\right) \geq z_{1,k}, & (20a) \\ \log_{2}\left(B_{k} + \sum_{m=1}^{M} P_{m} |\bar{h}_{m,l,k}|^{2}\right) \leq z_{2,k}, & (20b) \end{cases}$$

$$\begin{cases}
R_{E,k} \Leftrightarrow \log_2\left(A_{E,k} + B_{E,k} + \sum_{m=1}^M P_m \left| \boldsymbol{\omega}_E^H \bar{\mathbf{h}}_{m,IE} \right|^2\right) \\
& \leq z_{3,k}, \qquad (21a) \\
\log_2\left(B_{E,k} + \sum_{m=1}^M P_m \left| \boldsymbol{\omega}_E^H \bar{\mathbf{h}}_{m,IE} \right|^2\right) \geq z_{4,k}, \qquad (21b)
\end{cases}$$

which convert the objective into the expression  $z_{1,k} - z_{2,k}$  –  $z_{3,k} + z_{4,k}$  with the new constraints (20a)–(21b). However, these constraints are still non-convex. Hence, we again

4771

**VOLUME 5. 2024** 

introduce new auxiliary variables  $\Omega_r = \{r_{1,k}, r_{2,k}, r_{3,k}, r_{4,k}\},\$ which results in

$$\widetilde{R}_{k} \Leftrightarrow
\begin{cases}
\log_{2}(r_{1,k}) \geq z_{1,k}, & (22a) \\
A_{k} + B_{k} + \sum_{m=1}^{M} P_{m} |\bar{h}_{m,I,k}|^{2} \geq r_{1,k}, & (22b) \\
\log_{2}(r_{2,k}) \leq z_{2,k}, & (22c) \\
B_{k} + \sum_{m=1}^{M} P_{m} |\bar{h}_{m,I,k}|^{2} \leq r_{2,k}, & (22d)
\end{cases}$$

and

and
$$\widetilde{R_{E,k}} \Leftrightarrow \begin{cases}
\log_2(r_{3,k}) \leq z_{3,k}, & (23a) \\
A_{E,k} + B_{E,k} + \sum_{m=1}^M P_m \left| \boldsymbol{\omega}_E^H \bar{\mathbf{h}}_{m,IE} \right|^2 \leq r_{3,k}, & (23b) \\
\log_2(r_{4,k}) \geq z_{4,k}, & (23c) \\
B_{E,k} + \sum_{m=1}^M P_m \left| \boldsymbol{\omega}_E^H \bar{\mathbf{h}}_{m,IE} \right|^2 \geq r_{4,k}. & (23d)
\end{cases}$$

Again, constraints (22c) and (23a) are non-convex, which can be approximated using first order Taylor approximation at feasible points as in the following

$$\log_2\left(\tilde{r}_{2,k}^{(t)}\right) + \frac{\left(r_{2,k} - \tilde{r}_{2,k}^{(t)}\right)}{\tilde{r}_{2,k}^{(t)}\ln(2)} \le z_{2,k},\tag{24}$$

$$\log_2\left(\tilde{r}_{3,k}^{(t)}\right) + \frac{\left(r_{3,k} - \tilde{r}_{3,k}^{(t)}\right)}{\tilde{r}_{3,k}^{(t)}\ln(2)} \le z_{3,k},\tag{25}$$

And to deal with constraint (19), we introduce the set of auxiliary variables  $\gamma_m, \forall m \in \mathcal{M}$ , which relax the fraction into the following

$$P_m \left| \boldsymbol{\omega}_{B,m}^H \bar{\mathbf{h}}_{m,IS} \right|^2 \ge \gamma_m \bar{R}_{UL}^{th}, \tag{26}$$

$$\sum_{m' \neq m} P_{m'} \left| \boldsymbol{\omega}_{B,m}^{H} \bar{\mathbf{h}}_{m',IS} \right|^{2} + D_{m} \leq \gamma_{m}. \tag{27}$$

Finally, the overall UL power optimization problem can be reformulated as

Maximize Min 
$$z_{1,k} - z_{2,k} - z_{3,k} + z_{4,k}$$
, (28a)

subject to:

which can be solved using standard convex optimization

# 

Assuming  $\{v_k\}$ , w,  $\{\omega_{B,m}\}$  and  $\{P_m\}$  are given, we investigate the passive RIS beamforming optimization problem. To facilitate the discussion, we recast the terms within the signaling model in terms of  $\Theta$ . For example, the received signal at PU k from the PBS in (1a) can be expressed as

$$(\mathbf{h}_{P,k}^{H} + \mathbf{h}_{I,k}^{H} \mathbf{\Theta} \mathbf{H}_{P,I}) \mathbf{v}_{k} = \mathbf{h}_{P,k}^{H} \mathbf{v}_{k} + \mathbf{\theta}^{H} \operatorname{diag}(\mathbf{H}_{P,I} \mathbf{v}_{k})$$
$$\times \mathbf{h}_{I,k} = \left[1, \mathbf{\theta}^{H}\right] \left[\mathbf{h}_{P,k}^{H} \mathbf{v}_{k}; \operatorname{diag}(\mathbf{H}_{P,I} \mathbf{v}_{k}) \mathbf{h}_{I,k}\right] = \mathbf{\psi} \mathbf{g}_{P,k},$$

where  $\psi = [1, \boldsymbol{\theta}^H] \in \mathbb{C}^{1 \times (L+1)}$  and  $\boldsymbol{g}_{P,k} = [\boldsymbol{h}_{P,k}^H \boldsymbol{v}_k; \operatorname{diag}(\boldsymbol{H}_{P,l} \boldsymbol{v}_k) \boldsymbol{h}_{l,k}] \in \mathbb{C}^{(L+1) \times 1}$ . Therefore, the useful signal power can be expressed as

$$\left| \boldsymbol{\psi} \boldsymbol{g}_{P,k} \right|^2 = \boldsymbol{\psi} \boldsymbol{g}_{P,k} \boldsymbol{g}_{P,k}^H \boldsymbol{\psi}^H = \operatorname{Tr} (\boldsymbol{G}_{P,k} \boldsymbol{\Psi}),$$

(24) where  $\mathbf{G}_{P,k} = \mathbf{g}_{P,k} \mathbf{g}_{P,k}^H \in \mathbb{C}^{(L+1)\times(L+1)}$  and  $\mathbf{\Psi} = \mathbf{\psi}^H \mathbf{\psi} \in \mathbb{C}^{(L+1)\times(L+1)}$ . Similarly, the effective interuser interference channel can be defined as  $g_{PV} =$  $[\boldsymbol{h}_{P,k}^{H}\boldsymbol{v}_{k'}; \operatorname{diag}(\boldsymbol{H}_{P,l}\boldsymbol{v}_{k'})\boldsymbol{h}_{l,k}],$  which yields the following expression for the inter-user interference power

$$|\boldsymbol{\psi}\boldsymbol{g}_{P,k'}|^2 = \boldsymbol{\psi}\boldsymbol{g}_{P,k'}\boldsymbol{g}_{P,k'}^H\boldsymbol{\psi}^H = \operatorname{Tr}(\boldsymbol{G}_{P,k'}\boldsymbol{\Psi}).$$

In addition, the UL and AJ interference channels can be denoted as  $\mathbf{f}_{m,k} = [h_{m,k}; \operatorname{diag}(\mathbf{h}_{m,l})\mathbf{h}_{l,k}]$  with  $|\psi \mathbf{f}_{m,k}|^2 =$  $\operatorname{Tr}(\boldsymbol{F}_{m,k}\boldsymbol{\Psi})$  and  $\boldsymbol{e}_{S,k} = [\boldsymbol{h}_{S,k}^H\boldsymbol{w}; \operatorname{diag}(\boldsymbol{H}_{S,l}\boldsymbol{w})\boldsymbol{h}_{l,k}]$  with  $|\psi e_{S,k}|^2 = \text{Tr}(E_{S,k}\Psi)$ , respectively. Based on the above reformulations, the achievable SINR at PU k can be given as shown in (29a) on bottom of the page.

Similarly, for the signal received at Eve in (1b), the effective channel of the intercepted signal can be written as  $\mathbf{g}_{PE,k} = [\boldsymbol{\omega}_E^H \boldsymbol{H}_{P,E}^H \boldsymbol{v}_k; \operatorname{diag}(\boldsymbol{H}_{P,I} \boldsymbol{v}_k) \boldsymbol{H}_{I,E} \boldsymbol{\omega}_E],$ 

$$SINR_{k}(\boldsymbol{\Psi}) = \frac{Tr(\boldsymbol{G}_{P,k}\boldsymbol{\Psi})}{\sum_{k'\neq k} Tr(\boldsymbol{G}_{P,k'}\boldsymbol{\Psi}) + \sum_{m=1}^{M} P_{m}Tr(\boldsymbol{F}_{m,k}\boldsymbol{\Psi}) + Tr(\boldsymbol{E}_{S,k}\boldsymbol{\Psi}) + \sigma_{k}^{2}},$$
(29a)

$$SINR_{E,k}(\boldsymbol{\Psi}) = \frac{Tr(\boldsymbol{G}_{PE,k}\boldsymbol{\Psi})}{\sum_{k \neq k'} Tr(\boldsymbol{G}_{PE,k'}\boldsymbol{\Psi}) + \sum_{m=1}^{M} P_m Tr(\boldsymbol{F}_{m,E}\boldsymbol{\Psi}) + Tr(\boldsymbol{E}_{SE}\boldsymbol{\Psi}) + \tilde{\sigma}_E},$$
(29b)

$$SINR_{m}(\boldsymbol{\Psi}) = \frac{P_{m}Tr(\boldsymbol{F}_{S,m}\boldsymbol{\Psi})}{\sum_{m' \neq m} P_{m'}Tr(\boldsymbol{F}_{S,m'}\boldsymbol{\Psi}) + \sum_{k=1}^{K} Tr(\boldsymbol{G}_{k,m}\boldsymbol{\Psi}) + Tr(\boldsymbol{E}_{SS,m}\boldsymbol{\Psi}) + \tilde{\sigma}_{B,m}}.$$
 (29c)

the PUs interference channel can be written  $\mathbf{g}_{PE,k'} = [\boldsymbol{\omega}_E^H \boldsymbol{H}_{P,E}^H \boldsymbol{v}_{k'}; \operatorname{diag}(\boldsymbol{H}_{P,I} \boldsymbol{v}_{k'}) \boldsymbol{H}_{I,E} \boldsymbol{\omega}_E], \text{ the UL}$ interference of the SUs can be denoted by  $f_{m,E}$  $[\boldsymbol{\omega}_{E}^{H}\boldsymbol{h}_{m}^{H}]_{E}$ ; diag $(\boldsymbol{h}_{m,I})\boldsymbol{H}_{I,E}\boldsymbol{\omega}_{E}$ , the AJ signal effective channel can be denoted by  $\mathbf{e}_{SE} = [\mathbf{H}_{SF}^H \mathbf{w}; \operatorname{diag}(\mathbf{H}_{S,I} \mathbf{w}) \mathbf{H}_{I,E} \boldsymbol{\omega}_E]$  and finally, the AWGN noise is  $\tilde{\sigma}_E = \sigma_E^2 \| \boldsymbol{\omega}_E^H \|^2$ . Casting the corresponding powers in the form of a trace as mentioned above, the SINR at Eve can be given by (29b), also on bottom of the previous page. Accordingly, the achievable SR performance of PU k can be evaluated as  $\widehat{SR}_k(\Psi) \triangleq$  $\max_{k} \{ \log(1 + SINR_k(\boldsymbol{\Psi})) - \log(1 + SINR_{E_k}(\boldsymbol{\Psi})), 0 \}.$ 

Regarding the received SINR at the SBS due to the m-th user, we first notice that the received signal power of the  $m^{th}$  SU expressed in the numerator of (2b) is given by  $P_m |\boldsymbol{\omega}_{B,m}^H \bar{\boldsymbol{h}}_{m,IS}|^2 = P_m \boldsymbol{\omega}_{B,m}^H \bar{\boldsymbol{h}}_{m,IS} \bar{\boldsymbol{h}}_{m,IS}^H \boldsymbol{\omega}_{B,m}$ , where the corresponding effective channel is

$$\boldsymbol{\omega}_{B,m}^{H} \bar{\boldsymbol{h}}_{m,IS} = \boldsymbol{\omega}_{B,m}^{H} \boldsymbol{h}_{m,S}^{H} + \boldsymbol{\omega}_{B,m}^{H} \boldsymbol{H}_{I,S}^{H} \boldsymbol{\Theta} \boldsymbol{h}_{m,I}$$

$$= \boldsymbol{\omega}_{B,m}^{H} \boldsymbol{h}_{m,S}^{H} + \boldsymbol{\theta}^{H} \operatorname{diag}(\boldsymbol{h}_{m,I}) \boldsymbol{H}_{I,S} \boldsymbol{\omega}_{B,m}$$

$$= \left[1, \boldsymbol{\theta}^{H}\right] \left[\boldsymbol{\omega}_{B,m}^{H} \boldsymbol{h}_{m,S}^{H}; \operatorname{diag}(\boldsymbol{h}_{m,I}) \boldsymbol{H}_{I,S} \boldsymbol{\omega}_{B,m}\right]$$

$$= \boldsymbol{\psi} \boldsymbol{f}_{S,m}$$

with  $\mathbf{f}_{S,m} = [\boldsymbol{\omega}_{B,m}^H \boldsymbol{h}_{m,S}^H; \operatorname{diag}(\boldsymbol{h}_{m,I}) \boldsymbol{H}_{I,S} \boldsymbol{\omega}_{B,m}]$ . Hence, the numerator can now be expressed as

$$P_{m} \left| \boldsymbol{\omega}_{B,m}^{H} \bar{\boldsymbol{h}}_{m,IS} \right|^{2} = P_{m} \left| \boldsymbol{\psi} \boldsymbol{f}_{S,m} \right|^{2} = P_{m} \boldsymbol{\psi} \boldsymbol{f}_{S,m} \boldsymbol{f}_{S,m}^{H} \boldsymbol{\psi}^{H}$$
$$= P_{m} \operatorname{Tr} (\boldsymbol{F}_{S,m} \boldsymbol{\Psi}),$$

where  $\mathbf{F}_{S,m} = \mathbf{f}_{S,m} \mathbf{f}_{S,m}^H$ . Similar to the above, effective interference channels of other AJ can, respectively, be expressed PBS  $[\boldsymbol{\omega}_{B,m}^{H}\boldsymbol{h}_{m',S}^{H}; \operatorname{diag}(\boldsymbol{h}_{m',I})\boldsymbol{H}_{I,S}\boldsymbol{\omega}_{B,m}], \quad \boldsymbol{g}_{k,m}$  $[\boldsymbol{\omega}_{B,m}^{H}\boldsymbol{H}_{P,S}^{H}\boldsymbol{v}_{k};\operatorname{diag}(\boldsymbol{H}_{P,I}\boldsymbol{v}_{k})\boldsymbol{H}_{I,S}\boldsymbol{\omega}_{B,m}]$  and  $[\sqrt{\delta}\boldsymbol{\omega}_{B,m}^{H}\boldsymbol{H}_{S,S}^{H}\boldsymbol{w}; \operatorname{diag}(\boldsymbol{H}_{S,I}\boldsymbol{w})\boldsymbol{H}_{I,S}\boldsymbol{\omega}_{B,m}].$  This yields the expression in (29c), on bottom of the previous page, where  $\tilde{\sigma}_{B,m} = \sigma_B^2 \| \boldsymbol{\omega}_{B,m}^H \|^2$ .

Consequently, the RIS phase shift optimization problem can now be formulated in the SDP form as

$$\underset{\Psi}{\text{Maximize Min }} \widetilde{SR_k} \ (\Psi) \tag{30a}$$

subject to:

$$\log_2(1 + \text{SINR}_m(\boldsymbol{\Psi})) \ge R_{UL}^{\text{th}}, \forall m \in \mathcal{M}, \quad (30b)$$

$$\Psi_{l,l} = 1, \forall l \in \mathcal{L}, \quad \Psi \geq 0, \quad \text{Rank}(\Psi) = 1, (30c)$$

which is a non-convex optimization problem due to the objective and Rank-one constraint. Similar to the procedure in the active beamforming optimization problem, we relax the non-convexity of the objective (30a) by introducing new auxiliary variables  $\Omega_q = \{q_{1,k}, q_{2,k}, q_{3,k}, q_{4,k}\}$ , which results in

$$\begin{cases} \log_2(q_{1,k}) \ge p_{1,k}, \\ \operatorname{Tr}(\mathbf{G}_{P,k}\mathbf{\Psi}) + \sum_{k' \ne k} \operatorname{Tr}(\mathbf{G}_{P,k'}\mathbf{\Psi}) + \sigma_k^2 \end{cases}$$
(31a)

$$\widetilde{R}_{k} \Leftrightarrow \begin{cases}
+ \sum_{m=1}^{M} P_{m} \operatorname{Tr}(\boldsymbol{F}_{m,k} \boldsymbol{\Psi}) + \operatorname{Tr}(\boldsymbol{E}_{S,k} \boldsymbol{\Psi}) \geq q_{1,k}, & (31b) \\
\log_{2}(q_{2,k}) \leq p_{2,k}, & (31c) \\
\sum_{k' \neq k} \operatorname{Tr}(\boldsymbol{G}_{P,k'} \boldsymbol{\Psi}) + \sum_{m=1}^{M} P_{m} \operatorname{Tr}(\boldsymbol{F}_{m,k} \boldsymbol{\Psi})
\end{cases}$$

$$\log_2(q_{2,k}) \le p_{2,k},\tag{31c}$$

$$\sum_{k'\neq k} \operatorname{Tr}(\boldsymbol{G}_{P,k'}\boldsymbol{\Psi}) + \sum_{m=1}^{M} P_m \operatorname{Tr}(\boldsymbol{F}_{m,k}\boldsymbol{\Psi})$$

$$+\operatorname{Tr}(\boldsymbol{E}_{S,k}\boldsymbol{\Psi}) + \sigma_k^2 \le q_{2,k},\tag{31d}$$

and

$$\begin{cases} \log_2(q_{3,k}) \le p_{3,k}, \\ \operatorname{Tr}(\boldsymbol{G}_{PE,k}\boldsymbol{\Psi}) + \sum_{k \ne k'} \operatorname{Tr}(\boldsymbol{G}_{PE,k'}\boldsymbol{\Psi}) + \tilde{\sigma}_E \end{cases}$$
(32a)

$$\widetilde{R_{E,k}} \Leftrightarrow \begin{cases}
+ \sum_{m=1}^{M} P_m \operatorname{Tr}(\mathbf{F}_{m,E} \mathbf{\Psi}) + \operatorname{Tr}(\mathbf{E}_{SE} \mathbf{\Psi}) \leq q_{3,k}, (32b) \\
\log_2(q_{4,k}) \geq p_{4,k}, (32c) \\
\sum_{k \neq k'} \operatorname{Tr}(\mathbf{G}_{PE,k'} \mathbf{\Psi}) + \sum_{m=1}^{M} P_m \operatorname{Tr}(\mathbf{F}_{m,E} \mathbf{\Psi})
\end{cases}$$

$$\log_2(q_{4,k}) \ge p_{4,k}, \tag{32c}$$

$$\sum_{k} \operatorname{Tr}(\mathbf{F}_{k-k}, \mathbf{F}_{k-k}, \mathbf{F}_{k$$

$$\sum_{k \neq k'} \operatorname{Tr}(\mathbf{G}_{PE,k'}\mathbf{\Psi}) + \sum_{m=1} P_m \operatorname{Tr}(\mathbf{F}_{m,E}\mathbf{\Psi}) + \operatorname{Tr}(\mathbf{E}_{SE}\mathbf{\Psi}) + \tilde{\sigma}_E \ge q_{4,k}.$$
(32d)

equations pose Nevertheless, these non-convexity. Consequently, the SCA method is utilized to replace them with the subsequent upper bounds

$$\log_2(q_{2,k}) \le p_{2,k} \Rightarrow \log_2(\tilde{q}_{2,k}^{(t)}) + \frac{\left(q_{2,k} - \tilde{q}_{2,k}^{(t)}\right)}{\tilde{q}_{2,k}^{(t)} \ln(2)} \le p_{2,k},\tag{33}$$

$$\log_2(q_{3,k}) \le p_{3,k} \Rightarrow \log_2(\tilde{q}_{3,k}^{(t)}) + \frac{\left(q_{3,k} - \tilde{q}_{3,k}^{(t)}\right)}{\tilde{q}_{3,k}^{(t)} \ln(2)} \le p_{3,k}, \tag{34}$$

where  $\{\tilde{q}_{2,k}^{(t)}\}$  and  $\{\tilde{q}_{3,k}^{(t)}\}$  are feasible points at iteration t. In accordance with that, the phase shift optimization problem (30) is recast as

Maximize 
$$\min_{k} p_{1,k} - p_{2,k} - p_{3,k} + p_{4,k}$$
 (35a)

subject to:

(35b)

$$\operatorname{Tr}(\boldsymbol{F}_{S,m}\boldsymbol{\Psi}) \geq \frac{2^{R_{UL}^{\text{th}}} - 1}{P_m} \left( \sum_{m' \neq m} P_{m'} \operatorname{Tr}(\boldsymbol{F}_{S,m'}\boldsymbol{\Psi}) \right)$$

$$+\sum_{k=1}^{K}\operatorname{Tr}(\boldsymbol{G}_{k,m}\boldsymbol{\Psi})+\operatorname{Tr}(\boldsymbol{E}_{SS,m}\boldsymbol{\Psi})+\tilde{\sigma}_{B,m}), \forall m \in \mathcal{M},$$

(35c)

$$[\Psi]_{l,l} = 1, \forall l \in \mathcal{L},\tag{35d}$$

$$\Psi \succcurlyeq 0, \tag{35e}$$

**VOLUME 5. 2024** 4773

# Algorithm 1 Overall Optimization Algorithm

- 1: Set the initial values  $\boldsymbol{V}_{k}^{0}, \boldsymbol{W}^{0}, \boldsymbol{\omega}_{Rm}^{0}, \boldsymbol{\Psi}^{0}, P_{m}^{0}, \boldsymbol{\omega}_{E}^{0}$  and iteration index t = 1.
- 2: repeat
- 3:
- Obtain  $\boldsymbol{\omega}_{B,m}^{(t)}$  by solving (4).

  Optimize  $\boldsymbol{V}_{k}^{(t)}$  and  $\boldsymbol{W}^{(t)}$  by solving (16).

  Update  $P_{m}^{(t)}$  using (28). 4:
- 5:
- Optimize  $\Psi^{(t)}$  by solving (35). 6:
- t = t + 1. 7:
- 8: until Convergence

which is a relaxed SDP that can be solved using standard convex optimization toolboxes. When the optimal solution is not Rank-one, Gaussian randomization [33], [34] can be applied and the corresponding phase shift vector is constructed as  $\theta_l = e^{j \angle ([\psi]_{l+1}/[\psi]_1)}, \forall l \in \mathcal{L}$ .

# E. OVERALL OPTIMIZATION FRAMEWORK

Algorithm 1 summarizes the overall proposed solution approach, where the DL beamformers at the PBS, the DL iamming beamforming matrix, the UL receive beamforming at the FD-SBS, the UL transmit power and RIS phase shifts are alternatingly optimized until convergence.

# 1) CONVERGENCE ANALYSIS

The objective in (3a) represents the upper bound on the worst-case secrecy rate performance, i.e.,  $\bar{R}(V_k, \mathbf{W}, \mathbf{\Psi}, \boldsymbol{\omega}_{B.m}, P_m) \triangleq \text{Min SR}_k$ . This function is logarithmic in nature and exhibits a monotonically increasing behavior. Based on the findings of [35] and [36], the step 4 of the Algorithm 1, the optimal values of  $\mathbf{V}_k^{(t)}$  and  $\mathbf{W}^{(t)}$  at iteration t are obtained via  $\mathbf{\Psi}^{(t-1)}$ ,  $P_m^{(t-1)}$  and  $\boldsymbol{\omega}_{B,m}^{(t-1)}$  of the previous iteration. Hence, the following inequality holds

$$\bar{R}\left(\boldsymbol{V}_{k}^{(t-1)}, \boldsymbol{W}^{(t-1)}, \boldsymbol{\omega}_{B,m}^{(t-1)}, \boldsymbol{\Psi}^{(t-1)}, P_{m}^{(t-1)}\right) \\
\leq \bar{R}\left(\boldsymbol{V}_{k}^{(t)}, \boldsymbol{W}^{(t)}, \boldsymbol{\omega}_{B,m}^{(t-1)}, \boldsymbol{\Psi}^{(t-1)}, P_{m}^{(t-1)}\right)$$
(36)

Similarly, the other optimization variables stratify the following inequalities

$$\bar{R}\left(\boldsymbol{V}_{k}^{(t-1)}, \boldsymbol{W}^{(t-1)}, \boldsymbol{\omega}_{B,m}^{(t-1)}, \boldsymbol{\Psi}^{(t-1)}, P_{m}^{(t-1)}\right) \\
\leq \bar{R}\left(\boldsymbol{V}_{k}^{(t-1)}, \boldsymbol{W}^{(t-1)}, \boldsymbol{\omega}_{B,m}^{(t-1)}, \boldsymbol{\Psi}^{(t)}, P_{m}^{(t-1)}\right), \quad (37) \\
\bar{R}\left(\boldsymbol{V}_{k}^{(t-1)}, \boldsymbol{W}^{(t-1)}, \boldsymbol{\omega}_{B,m}^{(t-1)}, \boldsymbol{\Psi}^{(t-1)}, P_{m}^{(t-1)}\right) \\
\leq \bar{R}\left(\boldsymbol{V}_{k}^{(t-1)}, \boldsymbol{W}^{(t-1)}, \boldsymbol{\omega}_{B,m}^{(t)}, \boldsymbol{\Psi}^{(t-1)}, P_{m}^{(t-1)}\right), \quad (38) \\
\bar{R}\left(\boldsymbol{V}_{k}^{(t-1)}, \boldsymbol{W}^{(t-1)}, \boldsymbol{\omega}_{B,m}^{(t-1)}, \boldsymbol{\Psi}^{(t-1)}, P_{m}^{(t-1)}\right) \\
\leq \bar{R}\left(\boldsymbol{V}_{k}^{(t-1)}, \boldsymbol{W}^{(t-1)}, \boldsymbol{\omega}_{B,m}^{(t-1)}, \boldsymbol{\Psi}^{(t-1)}, P_{m}^{(t)}\right), \quad (39)$$

From (36)–(39), we have

$$\bar{R}\left(\boldsymbol{V}_{k}^{(t-1)}, \boldsymbol{W}^{(t-1)}, \boldsymbol{\omega}_{B,m}^{(t-1)}, \boldsymbol{\Psi}^{(t-1)}, P_{m}^{(t-1)}\right) \\
\leq \bar{R}\left(\boldsymbol{V}_{k}^{(t)}, \boldsymbol{W}^{(t)}, \boldsymbol{\omega}_{B,m}^{(t)}, \boldsymbol{\Psi}^{(t)}, P_{m}^{(t)}\right). \tag{40}$$

The inequality in (40) demonstrates that the objective function  $\bar{R}$  consistently remains non-decreasing after each iteration. Consequently, Algorithm 1 is assured to converge.

# 2) COMPLEXITY ANALYSIS

we analyze the computation complexity of the proposed solution in Algorithm 1. According to [37], The complexity of the receive beamforming and UL power problems is given by  $\mathcal{O}(N_r^3 + M^3)$  due to the matrix inversion in (5) and the SCA process. Moreover, the computational complexity imposed by the SDP<sup>3</sup> sub-problems are  $\mathcal{O}((N_t N_e)^{3.5}$  +  $(N_p K)^{3.5}$ ) for the active beamforming problem and  $\mathcal{O}((L +$ 1)<sup>3.5</sup>) for the passive beamforming one. Therefore, the overall complexity is found as  $\mathcal{O}(\ell(N_r^3 + M^3 + (N_t N_e)^{3.5} +$  $(N_p K)^{3.5} + (L+1)^{3.5}$ ), where  $\ell$  symbolizes the number of iterations required for convergence.

### V. SIMULATION RESULTS

Through this section, we present simulation results to validate the effectiveness of our proposed approach. All simulation results are averaged over 1000 channel realizations. The following parameters are set as default unless otherwise stated. We consider the locations, with respect to the origin, of the PBS, the FD-SBS, the RIS and Eve as (0, 0), (300, 0), (200, 0) and (250, 50), respectively. The PBS is equipped with  $N_p = 4$  antennas, while the FD-SBS has  $N_t = N_r = 4$ antennas, Eve has  $N_e = 2$  antennas and the RIS is equipped with L = 32 elements. Moreover, the PUs and SUs are single antenna legitimate users. Two PUs and two SUs are assumed uniformly distributed in two disks each of radius 15 m with centers at (150, 30) and (330, 40), respectively. At the reference distance of 1 meter, a pathloss of 30 dB is assumed and the background noise power is -80 dBm. The direct communication channels face a path-loss exponent of 3.9 with Rayleigh fading, whereas channels associated with the RIS encounter a path-loss exponent of 2.1 with Rician factor  $\kappa = 5$  dB. The SI channel follows the Rayleigh distribution with cancellation factor -130 dB [39]. The transmit powers of the PBS, FD-SBS and SUs are set to 30 dBm, 25 dBm and 10 dBm, respectively.

Fig. 2 shows the convergence of the proposed solution against the iterations. It is clear that the proposed scheme converges to a non-increasing secrecy performance, where no further improvement can be achieved within about 14 iterations. Furthermore, the proposed solution is compared with two benchmark schemes, namely "no RIS" and "rand RIS", where the former refers to a system with no RIS while the latter refers to one deploying an RIS with random phase shifts. Clearly, the proposed solution outperforms the "no RIS" case by 24.7%, while the cases of "no RIS"

<sup>3</sup>In our work, we utilized SDP to solve the RIS phase shift optimization problem, employing CVX-based convexification method to address complex constraints inherent in our specific problem setup. As highlighted in [38], on page 896, left column, while SDP-based methods are known to be more time-consuming, they offer greater flexibility in handling complex constraints such as quality of service (QoS) requirements.

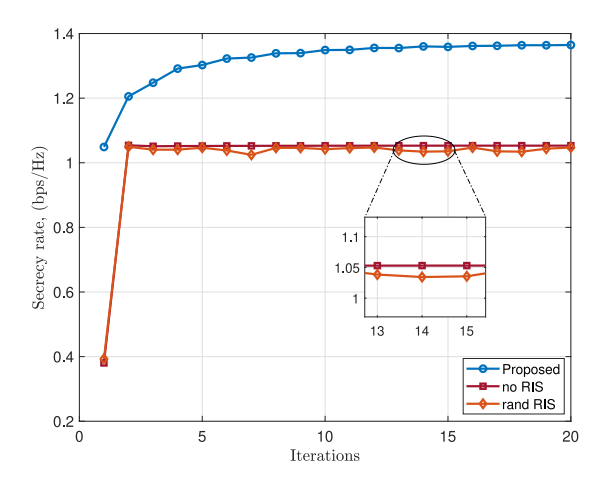


FIGURE 2. Secrecy rate convergence

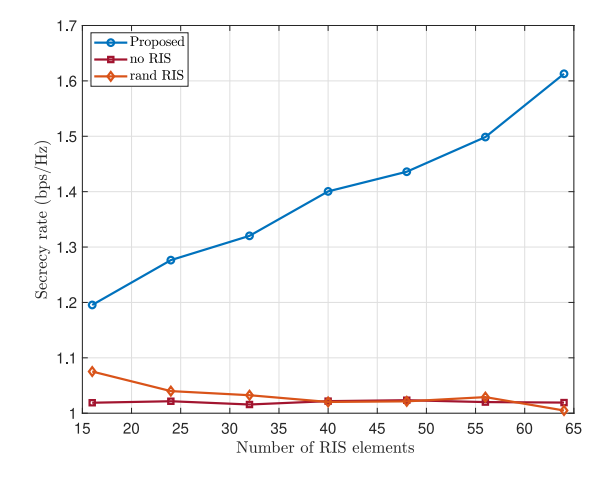
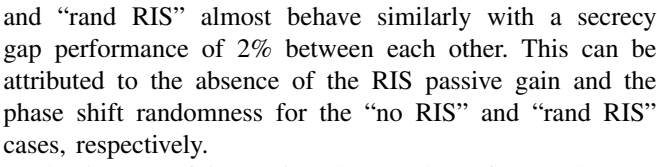


FIGURE 3. Secrecy rate performance versus the number of RIS elements.



The impact of increasing the number of RIS elements on the secrecy rate performance is depicted in Fig. 3. The performance of the proposed system shows a 33% improvement in the secrecy rate when the number of RIS elements increases from 16 to 64. Furthermore, the performance gap between the "no RIS" case and the proposed system grows with the number of RIS elements, where the "no RIS" exhibits a flat secrecy performance. On the other hand, an RIS with random phase shift deteriorates the secrecy rate when the number of RIS elements increases by 6%. According to this discussion, we conclude the following. First, the optimization of RIS phase shift plays a crucial role against the potential Eve. Second, random RIS phase shifts may leak legitimate information that affects the security of communication system.

Next, we investigate Eve's location as it approaches the FD-SBS and the RIS in Fig. 4. Obviously, moving Eve

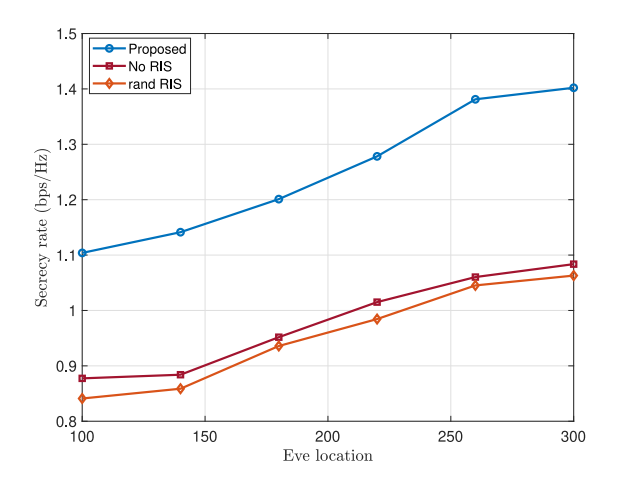


FIGURE 4. Impact of Eve's location on the secrecy rate.

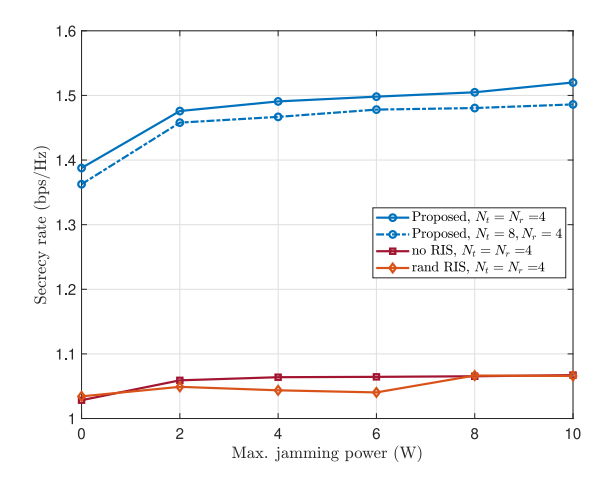


FIGURE 5. The secrecy rate against the maximum jamming power budget.

towards the FD-SBS improves the secrecy performance, where the RIS passively beamforms the jamming signal to degrade the received SINR at Eve. Specifically, the proposed solution achieves 19.5% and 23.1% secrecy improvement over the "no RIS" and 'rand RIS" cases, respectively, when the location of Eve becomes (220, 50).

Fig. 5 illustrates the effect of the maximum allowed jamming power on the secrecy rate performance. The proposed solution shows enhanced secrecy rate in comparison to the benchmark schemes, where the proposed scheme outperforms the "no RIS" case by 41.5% when  $N_t = N_r = 4$ and  $P_z^{\text{max}} = 6$  W. Moreover, the performance drops by 1.35% when the number of transmitting antennas at the FD-SBS increases from 4 to 8. This is because although the increase in  $N_t$  may improve the jamming gain towards Eve, it also adds interference to the received signal at the PU. Also, the "no RIS" and "rand RIS" cases almost converge to the same secrecy values as  $P_{\tau}^{\text{max}} \geq 8 \text{ W}$  due to the saturation of the beamformers to the maximum allowed levels, i.e.,  $\operatorname{Tr}(\boldsymbol{W}) = P_z^{\max}$  and  $\sum_{k=1}^K \operatorname{Tr}(\boldsymbol{V}_k) = P_{DL}^{\max}$ . This is to keep balance between the jamming gain and the signal quality requirement for PU communication.

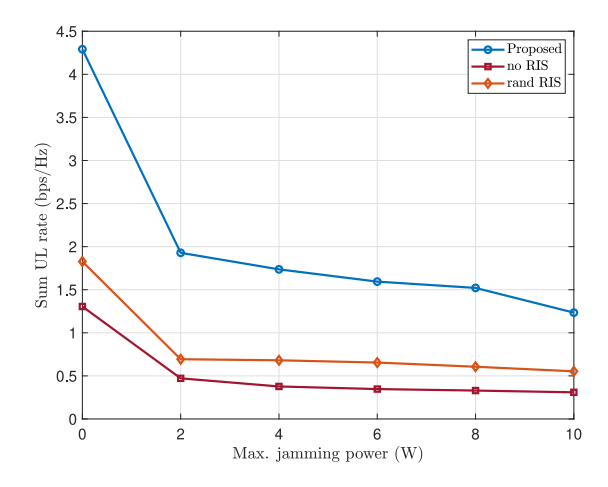


FIGURE 6. The sum UL rate against the maximum jamming power budget.

Finally, we examine the achievable UL communication rate of the secondary network against the maximum jamming power in Fig. 6. The UL rate of the SUs decreases as the jamming power increases due to the added self-interference at the FD-SBS. Again, we observe that the proposed scheme outperforms the benchmark schemes. However, increasing the value of  $P_z^{\text{max}}$  is not always useful, where it deteriorates the UL QoS requirements. For instance, the UL rate of the proposed solution decreases by about 3 bps/Hz, while the "no RIS" and "rand RIS" cases lose about 1 and 1.3 bps/Hz, respectively, across the range of  $P_z^{\text{max}}$ . To further explain, the direct path between the SUs and the FD-SBS dominates the self-interference term in the "no RIS" case, while the existence of the RIS enhances the same term via the passive gain in case of the proposed scheme and the "rand RIS" case. Furthermore, it is observed that increasing  $P_{\tau}^{\max}$  to a value greater than or equal to 2 W improves the secrecy rate as in Fig. 5, but it concurrently results in a drop in the UL communication rate. Therefore, the value  $P_z^{\text{max}}$  should be carefully tuned in order to balance the secure operation of the primary network and the UL communication requirements of the secondary network.

# VI. CONCLUSION

In this paper, we investigated the application of RIS in enhancing the security of MU-SIMO full-duplex cognitive radio network, where FD-SBS employs jamming attacks to thwart eavesdropping attempts. Our investigation encompasses the PBS DL beamforming, SBS AJ, passive RIS beamforming and the UL communication power, with a focus on achieving the balance between the optimal security performance and UL service requirement. To address this, we introduce an alternating optimization algorithm, in which semidefinite program (SDP) and successive convex approximation (SCA) techniques are employed. The simulation indicates that the optimization of RIS phase shift is crucial in countering potential eavesdropping, where shifting the Eve towards the FD-SBS and RIS enhances secrecy performance through passive beamforming of the RIS.

Moreover, the proposed solution consistently outperforms benchmark schemes in terms of secrecy rate. However, an increase in transmitting antennas at FD-SBS introduces a trade-off between jamming gain towards Eve and interference to the primary user (PU) signal. Additionally, careful tuning of the jamming power is essential to balance secure primary network operation and uplink communication requirements of the secondary network. In future work, we would like to further investigate the feasibility of adopting a two-timescale design scheme for secure transmission design of the RIS-aided FD-CR systems. At that time, we can balance such a trade-off on the performance-overhead, further contributing to the practicability and efficiency of our system.

### **REFERENCES**

- W. Zhang, C.-X. Wang, X. Ge, and Y. Chen, "Enhanced 5G cognitive radio networks based on spectrum sharing and spectrum aggregation," *IEEE Trans. Commun.*, vol. 66, no. 12, pp. 6304–6316, Dec. 2018.
- [2] X. Wu, J. Ma, Z. Xing, C. Gu, X. Xue, and X. Zeng, "Secure and energy efficient transmission for IRS-assisted cognitive radio networks," *IEEE Trans. Cogn. Commun. Netw.*, vol. 8, no. 1, pp. 170–185, Mar. 2022.
- [3] Z. Lin, M. Lin, B. Champagne, W.-P. Zhu, and N. Al-Dhahir, "Secrecy-energy efficient hybrid beamforming for satellite-terrestrial integrated networks," *IEEE Trans. Commun.*, vol. 69, no. 9, pp. 6345–6360, Sep. 2021.
- [4] Z. Lin, M. Lin, T. De Cola, J.-B. Wang, W.-P. Zhu, and J. Cheng, "Supporting IoT with rate-splitting multiple access in satellite and aerial-integrated networks," *IEEE Internet Things J.*, vol. 8, no. 14, pp. 11123–11134, Jul. 2021.
- [5] X. Wu, J. Ma, C. Gu, X. Xue, and X. Zeng, "Robust secure transmission design for IRS-assisted mmwave cognitive radio networks," *IEEE Trans. Veh. Technol.*, vol. 71, no. 8, pp. 8441–8456, Aug. 2022.
- [6] A. D. Wyner, "The wire-tap channel," Bell Syst. Tech. J., vol. 54, no. 8, pp. 1355–1387, Oct. 1975.
- [7] Y. He, J. Evans, and S. Dey, "Secrecy rate maximization for cooperative overlay cognitive radio networks with artificial noise," in *Proc. IEEE Int. Conf. Commun. (ICC)*, 2014, pp. 1663–1668.
- [8] V.-D. Nguyen, T. M. Hoang, and O.-S. Shin, "Secrecy capacity of the primary system in a cognitive radio network," *IEEE Trans. Veh. Technol.*, vol. 64, no. 8, pp. 3834–3843, Aug. 2015.
- [9] V.-D. Nguyen, T. Q. Duong, O.-S. Shin, A. Nallanathan, and G. K. Karagiannidis, "Enhancing PHY security of cooperative cognitive radio multicast communications," *IEEE Trans. Cogn. Commun. Netw.*, vol. 3, no. 4, pp. 599–613, Dec. 2017.
- [10] P. X. Nguyen, H. V. Nguyen, V.-D. Nguyen, and O.-S. Shin, "UAV-enabled jamming noise for achieving secure communications in cognitive radio networks," in *Proc. 16th IEEE Annu. Consum. Commun. Netw. Conf. (CCNC)*, 2019, pp. 1–6.
- [11] X. He, X. Li, H. Ji, and H. Zhang, "Resource allocation for secrecy rate optimization in UAV-assisted cognitive radio network," in *Proc. IEEE Wireless Commun. Netw. Conf. (WCNC)*, 2021, pp. 1–6.
- [12] Y. Wang, L. Chen, Y. Zhou, X. Liu, F. Zhou, and N. Al-Dhahir, "Resource allocation and trajectory design in UAV-assisted jamming wideband cognitive radio networks," *IEEE Trans. Cogn. Commun. Netw.*, vol. 7, no. 2, pp. 635–647, Jun. 2021.
- [13] Z. Lin et al., "Refracting RIS-aided hybrid satellite-terrestrial relay networks: Joint beamforming design and optimization," *IEEE Trans. Aerosp. Electron. Syst.*, vol. 58, no. 4, pp. 3717–3724, Aug. 2022.
- [14] K. An et al., "Exploiting multi-layer refracting RIS-assisted receiver for HAP-SWIPT networks," *IEEE Trans. Wireless Commun.*, early access, May 3, 2024, doi: 10.1109/TWC.2024.3394214.
- [15] S. Hong, C. Pan, H. Ren, K. Wang, and A. Nallanathan, "Artificial-noise-aided secure MIMO wireless communications via intelligent reflecting surface," *IEEE Trans. Commun.*, vol. 68, no. 12, pp. 7851–7866, Dec. 2020.
- [16] L. Dong, H.-M. Wang, and H. Xiao, "Secure cognitive radio communication via intelligent reflecting surface," *IEEE Trans. Commun.*, vol. 69, no. 7, pp. 4678–4690, Jul. 2021.

- [17] X. Wu, J. Ma, and X. Xue, "Joint beamforming for secure communication in RIS-assisted cognitive radio networks," J. Commun. Netw., vol. 24, no. 5, pp. 518-529, Oct. 2022.
- [18] Y. Sun, X. Jia, X. Han, M. Xie, and L. Zhang, "Physical layer securityoriented energy-efficient resource allocation and trajectory design for UAV jammer over 5G millimeter wave cognitive relay system," Trans. Emerg. Telecommun. Technol., vol. 35, no. 1, 2024, Art. no. e4915.
- [19] P. Hema and A. Babu, "Full-duplex jamming for physical layer security improvement in NOMA-enabled overlay cognitive radio networks," Secur. Priv., vol. 7, no. 3, p. e371, 2024
- [20] Q. Wu and R. Zhang, "Towards smart and reconfigurable environment: Intelligent reflecting surface aided wireless network," IEEE Commun. Mag., vol. 58, no. 1, pp. 106-112, Jan. 2020.
- [21] Q. Wu, S. Zhang, B. Zheng, C. You, and R. Zhang, "Intelligent reflecting surface-aided wireless communications: A tutorial," IEEE Trans. Commun., vol. 69, no. 5, pp. 3313-3351, May 2021.
- Requirements for Support of Radio Resource Management, 3GPP Standard TS 38.133, 2014.
- T. S. Rappaport, "Wireless communications-principles and practice,
- (the book end)," *Microw. J.*, vol. 45, no. 12, pp. 128–129, 2002. [24] H. Guo, Y.-C. Liang, J. Chen, and E. G. Larsson, "Weighted sum-rate maximization for reconfigurable intelligent surface aided wireless networks," IEEE Trans. Wireless Commun., vol. 19, no. 5, pp. 3064-3076, May 2020.
- [25] G. Zhou, C. Pan, H. Ren, K. Wang, and A. Nallanathan, "A framework of robust transmission design for IRS-aided MISO communications with imperfect cascaded channels," IEEE Trans. Signal Process., vol. 68, pp. 5092-5106, Aug. 2020.
- [26] H.-M. Wang, J. Bai, and L. Dong, "Intelligent reflecting surfaces assisted secure transmission without eavesdropper's CSI," IEEE Signal Process. Lett., vol. 27, pp. 1300-1304, Jul. 2020.
- [27] B. Feng, Y. Wu, M. Zheng, X.-G. Xia, Y. Wang, and C. Xiao, "Large intelligent surface aided physical layer security transmission," IEEE Trans. Signal Process., vol. 68, pp. 5276-5291, Sep. 2020.
- Z. Wang et al., "IRS-enhanced spectrum sensing and secure transmission in cognitive radio networks," IEEE Trans. Wireless Commun., early access, Mar. 5, 2024, doi: 10.1109/TWC.2024.3370812
- [29] K. Zhi, C. Pan, H. Ren, K. K. Chai, and M. Elkashlan, "Active RIS versus passive RIS: Which is superior with the same power budget?" IEEE Commun. Lett., vol. 26, no. 5, pp. 1150-1154, May 2022.
- [30] A. A. Salem, M. H. Ismail, and A. S. Ibrahim, "Active reconfigurable intelligent surface-assisted MISO integrated sensing and communication systems for secure operation," IEEE Trans. Veh. Technol., vol. 72, no. 4, pp. 4919-4931, Apr. 2023.
- [31] A. Ramezani-Kebrya, M. Dong, B. Liang, G. Boudreau, and S. H. Seyedmehdi, "Joint power optimization for device-to-device communication in cellular networks with interference control," IEEE Trans. Wireless Commun., vol. 16, no. 8, pp. 5131-5146, Aug. 2017.
- [32] M. Grant and S. Boyd. "CVX: MATLAB software for disciplined convex programming, version 2.1." 2014. [Online]. Available: https://cvxr.com/cvx/
- [33] M. Cui, G. Zhang, and R. Zhang, "Secure wireless communication via intelligent reflecting surface," IEEE Wireless Commun. Lett., vol. 8, no. 5, pp. 1410-1414, Oct. 2019.
- [34] A. A. Salem, A. S. Ibrahim, and M. H. Ismail, "An optimization framework for RIS-based energy-efficient multi-cell NOMA systems," Veh. Commun., vol. 43, Oct. 2023, Art. no. 100657.
- [35] K. Feng, X. Li, Y. Han, S. Jin, and Y. Chen, "Physical layer security enhancement exploiting intelligent reflecting surface," IEEE Commun. Lett., vol. 25, no. 3, pp. 734-738, Mar. 2021.
- [36] J. Chen, Y.-C. Liang, Y. Pei, and H. Guo, "Intelligent reflecting surface: A programmable wireless environment for physical layer security," IEEE Access, vol. 7, pp. 82599-82612, 2019.
- [37] A. Ben-Tal and A. Nemirovski, Lectures on Modern Convex Optimization: Analysis, Algorithms, and Engineering Applications. Philadelphia, PA, USA: SIAM, 2001.
- [38] C. Pan et al., "An overview of signal processing techniques for RIS/IRS-aided wireless systems," IEEE J. Sel. Topics Signal Process., vol. 16, no. 5, pp. 883-917, Aug. 2022.
- M. Elsayed, A. A. A. El-Banna, O. A. Dobre, W. Shiu, and P. Wang, "Hybrid-layers neural network architectures for modeling the self-interference in full-duplex systems," IEEE Trans. Veh. Technol., vol. 71, no. 6, pp. 6291-6307, Jun. 2022.



A. ABDELAZIZ SALEM received the M.Sc. and Ph.D. degrees in electronics and electrical communications engineering from the Faculty of Electronic Engineering, Menoufia University, Egypt, in 2015 and 2019, respectively. He is currently a Postdoctoral Research Fellow with the University of Sharjah. He is also an Assistant Professor with the Department of Electronics and Electrical Communications Engineering, Menoufia University. His research interests include applying convex optimization approaches on ultra-dense

networks, vehicular communications, intelligent reflecting surface assisted communications, non-orthogonal multiple access, and game theory applications.



MAHMOUD H. ISMAIL (Senior Member, IEEE) received the B.Sc. degree (with Highest Hons.) in electronics and electrical communications engineering and the M.Sc. degree in communications engineering from Cairo University, Egypt, in 2000 and 2002, respectively, and the Ph.D. degree in electrical engineering from the University of Mississippi, MS, USA, in 2006. From August 2000 to August 2002, he was a Research and Teaching Assistant with the Department of Electronics and Electrical Communications

Engineering, Cairo University. From 2004 to 2006, he was a Research Assistant with the Center for Wireless Communications, University of Mississippi. He is currently a Full Professor with the American University of Sharjah, Sharjah, UAE, and a Full Professor (on leave) with the Department of Electronics and Electrical Communications Engineering, Cairo University. He was also a Systems Engineering Consultant with Newport Media Inc. (currently part of Microchip), Cairo, from 2006 to 2014. His research is in the general area of wireless communications with emphasis on performance evaluation of next-generation wireless systems and communications over fading channels. He is the recipient of the University of Mississippi Summer Assistantship Award in 2004 and 2005, the University of Mississippi Dissertation Fellowship Award in 2006, the University of Mississippi Graduate Achievement Award in Electrical Engineering in 2006, and the Best Paper Award presented at the 10th IEEE Symposium on Computers and Communications, La Manga del Mar Menor, Spain, in 2005.



AHMED S. IBRAHIM (Senior Member, IEEE) received the B.S. and M.S. degrees in electronics and electrical communications engineering from Cairo University, Cairo, Egypt, in 2002 and 2004, respectively, and the Ph.D. degree in electrical engineering from the University of Maryland at College Park, College Park, MD, USA, in 2009. He is currently an Associate Professor with the Electrical and Computer Engineering Department, Florida International University (FIU), Miami, FL. USA. Prior to joining FIU, he was an Assistant

Professor with Cairo University, a Wireless Research Scientist with Intel Corporation, and a Senior Engineer with Interdigital Communications Inc. His research interests span various topics of wireless systems including drone-assisted millimeter wave communications, vehicular communications, and rethinking wireless networks through the lens of Riemannian geometry. He is a recipient of the NSF CAREER Award in 2022.

**VOLUME 5. 2024** 4777